

AD-A215 712



S DTIC
 ELECTE
 DEC 27 1989 **D**
 B

STARING FOCAL PLANE
 ARRAY SYSTEM
 MODELING

THESIS

John Gerard Murphy
 Captain, USAF

AFIT/GEO/ENP/89D-3

DEPARTMENT OF THE AIR FORCE
 AIR UNIVERSITY
AIR FORCE INSTITUTE OF TECHNOLOGY

Wright-Patterson Air Force Base, Ohio

DISTRIBUTION STATEMENT A
 Approved for public release
 Distribution Unlimited

89 12 26 145

AFIT/GEO/ENP/89D-3

STARING FOCAL PLANE
ARRAY SYSTEM
MODELING

THESIS

Presented to the Faculty of the School of Engineering
of the Air Force Institute of Technology
Air University
In Partial Fulfillment of the
Requirements for the Degree of
Master of Science in Electrical Engineering

John Gerard Murphy, B.S., M.S.
Captain, USAF

December, 1989

Approved for public release; distribution unlimited.

Acknowledgments

I would like to thank Dr Ted Luke for suggesting the topic and guiding me along the way with patience and care. I would also like to thank Fred Blommel and the WRDC Electro-optics shop for their assistance and for providing the laboratory data used in this study. And thank you Laura for helping make it all go so smoothly.

John Gerard Murphy

Accession For	
NTIS GRA&I	<input checked="" type="checkbox"/>
DTIC TAB	<input type="checkbox"/>
Unannounced	<input type="checkbox"/>
Justification	
By _____	
Distribution/	
Availability Codes	
Dist	Avail and/or Special
A-1	

Table of Contents

	Page
Acknowledgments	ii
Table of Contents	iii
List of Figures	vi
List of Tables	vii
Abstract	viii
I. Introduction	1-1
1.1 Background	1-2
1.1.1 MRTD	1-2
1.1.2 MRTD in Modeling	1-3
1.1.3 MRTD Shortcomings	1-3
1.2 Problem Statement	1-4
1.3 Scope	1-5
1.4 Standards	1-5
1.5 General Approach	1-6
1.6 Thesis Organization	1-6
II. Relevant Background	2-1
2.1 Introduction	2-1
2.2 Focal Plane Arrays	2-1
2.2.1 Scanning Techniques	2-1
2.2.2 FPA Fabrication	2-2

	Page
2.3 Linear Systems	2-3
2.3.1 Sampled Imaging Systems	2-3
2.3.2 Isoplanarity	2-3
2.3.3 Aliasing	2-4
2.4 FPA Modeling	2-4
2.4.1 Sampling Effects	2-5
2.4.2 Detector Response	2-5
2.4.3 Transfer and Readout	2-6
2.4.4 Response Nonuniformity	2-6
2.5 FPA Figures of Merit	2-8
2.6 Improved MRTD Models	2-9
2.6.1 Second Generation Effects	2-9
2.6.2 Objective Standard	2-9
2.7 Staring Array MRTD Models	2-10
2.7.1 Eye/Brain Models	2-10
2.7.2 Aliasing	2-12
2.7.3 Nonuniformity Treatment	2-13
2.7.4 A Closer Look	2-14
2.8 Summary	2-15
III. Staring Array System Modeling	3-1
3.1 Introduction	3-1
3.2 Modeling Methodology	3-1
3.2.1 MRTD Functional Form	3-1
3.2.2 Modeling Process	3-1
3.2.3 Sensitivity Analysis	3-2
3.2.4 MTF Derivation	3-3
3.2.5 Temporal Integration	3-8

	Page
3.2.6 Spatial Integration	3-9
3.2.7 Threshold	3-10
3.3 MWIR-Modified NVL Model	3-10
3.3.1 NVL MRTD	3-11
3.3.2 Simpler Forms	3-12
3.4 Rosell Model	3-14
3.4.1 Rosell MRTD	3-14
3.4.2 Rosell NE Δ T	3-15
3.5 Kennedy Model	3-18
3.5.1 Kennedy MRTD	3-19
3.5.2 Kennedy Aliasing Treatment	3-20
3.6 Summary	3-23
IV. Model Comparisons	4-1
4.1 Introduction	4-1
4.2 Modeling Process	4-1
4.3 Camera-One Comparison	4-1
4.4 Camera-Two Comparison	4-3
4.5 Camera-Three Comparison	4-10
4.6 Summary	4-12
V. Conclusions and Recommendations	5-1
5.1 Conclusions	5-1
5.2 Recommendations	5-2
Bibliography	BIB-1
Vita	VITA-1

List of Figures

Figure	Page
3.1. MRTD Modeling Process	3-2
3.2. Typical Camera MTFs	3-6
3.3. Transforms of Infinite and 4-Bar Patterns	3-22
4.1. Camera-One Vertical MRTD Comparison	4-4
4.2. Camera-One Horizontal MRTD Comparison	4-5
4.3. Camera-Two Vertical MRTD Comparison	4-8
4.4. Camera-Two Horizontal MRTD Comparison	4-9
4.5. Camera-Three Vertical MRTD Comparison	4-13
4.6. Camera Three Horizontal MRTD Comparison	4-14

List of Tables

Table	Page
2.1. Staring Array Models	2-11
3.1. Basic MTF Expressions	3-3
4.1. Camera-One Parameter Listing	4-2
4.2. Camera-One Measured Values (52:7)	4-3
4.3. Camera-Two Parameter Listing	4-6
4.4. Camera-Two Measured Values (52:7)	4-6
4.5. Camera-Three Parameter Listing	4-10
4.6. Camera-Three Measured Values (53:14)	4-11
4.7. Model Performance	4-15

AFIT/GEO/ENP/89D-3

Abstract

This thesis analyzed the problems of modeling staring focal plane arrays. Two problem areas were highlighted; the difficulty in modeling the operator interface and the inadequate characterization of focal plane array noise sources. The effects of aliasing, response nonuniformity, and the two dimensional nature of the spatial and temporal noise require more sophisticated handling than found in present models. Three staring array models were used to predict the Minimum Resolvable Temperature Difference (MRTD) for three Platinum Silicide staring array cameras. The predictions were then compared, analyzed, and suggestions for model improvement were made.

STARING FOCAL PLANE ARRAY SYSTEM MODELING

I. Introduction

The theoretical base for thermal imaging modeling was developed during the Vietnam era and much of that base was borrowed from television models (1:74). Little has been done since to develop a theoretical foundation of thermal imaging system (TIS) modeling. Such models can be used to compare system performance of different TIS designs, identify critical parameters and material technologies that warrant more attention, and determine the operational suitability of TIS designs *prior* to development. The growing use of new detector/scanning concepts, particularly staring focal plane array (FPA) technology, introduce new parameters influencing system performance that are not adequately addressed by existing models (1:76). An effort within a NATO research working group (Panel 4 on Optics and Infrared) to assess the advanced IR modeling capability of member nations concluded that no analytical models now exist to adequately describe staring focal plane array system performance (2). The inadequacy of the present TIS models can lead to inadequate specifications and the acquisition of systems that don't meet operational requirements. We can't design and build better next generation thermal imaging systems if there is no generally accepted performance criterion upon which to base this improvement (3:264). More accurate and predictive (TIS) models are required to guide Air Force engineers and managers in advancing only the most promising new technologies.

1.1 Background

Evaluating TIS performance touches either directly (human observer) or indirectly (Automatic Target Recognition) on the subject of image quality. The difficulty in analyzing image quality in TIS models is perhaps conveyed best by the views of some experts in the field.

The problems inherent in characterizing image quality are ... "accentuated in thermal systems because thermal image contrasts don't look quite like the contrasts of a visible scene, so a mental set of standards such as we apply to commercial TV is difficult to acquire. We are very sensitive to changes in home television reproduction and in newspaper halftone photographs, but it is possible to overlook relatively serious degradations in FLIR image quality because of the somewhat unnatural appearance of even good imagery and the wide variations in system design which are customary." (4:182)

Much of the early work in characterizing image quality involved television images. Otto Schade, a significant contributor to this field, offers this advice for TIS designers:

The 'perfect' display is perhaps in a practical sense a piece of the real world shown on the screen which looks the same as the real world to the unaided eye, or, for a different spectral band (IR) 'appears' to be a piece of the real world, sharp and clear and without distortion. In the latter case we have no subjective quality equivalent because we cannot see the infrared world directly. Here we must establish an objective standard. (5:13)

Because spatial resolution and thermal sensitivity dominate FLIR performance, minimum resolvable temperature difference (MRTD) has evolved as the primary 'objective' standard in evaluating TIS systems.

1.1.1 MRTD The most useful and commonly used figure of merit for thermal imaging systems is the minimum resolvable temperature difference (MRTD) (6:179). "MRTD is a measure of the temperature difference at which a 4-bar target can just

be resolved, as a function of the bar spatial frequency." (7:268) A close analog to MRTD is the minimum detectable temperature difference (MDTD). Because MRTD combines both the spatial resolution and noise characteristics of the thermal imaging system, it represents an excellent summary measure (7:268). One of the strengths of MRTD, its subjective nature, is also one of its major drawbacks. The MRTD is measured by increasing the temperature difference between four bars (of certain spacing) and a constant temperature background until the bars can just be *resolved* by a trained observer. This procedure is repeated for various bar spacings (spatial frequencies). In this manner, MRTD not only combines measures of sensitivity and resolution, it also conveniently includes the *human factor* which is very difficult to model. However, because MRTD is a subjective measure, there are significant variations in MRTD results obtained by different operators (6:179). Moreover, since there is no established criterion for resolution, the competitive environment existing among contractors encourages the use of criterion which tends to artificially lower the MRTD, which in turn, further limits MRTD's usefulness (7:269).

1.1.2 MRTD in Modeling Notwithstanding the problems discussed above, MRTD has been used for years to analyze, compare, and predict the performance of TI Systems. In fact, the major thermal imaging system models used within the military community use MRTD to model the sensor's contribution to overall TIS performance. The Night Vision Laboratory Static Performance Model (NVLSPM) and the U.S. Army Missile Command (MICOM) Infrared Imaging System Performance Model (MIISPM), and the Army's Fire Control Sensor Simulator (FCSS) are examples of models that rely upon MRTD to account for the sensitivity and resolution of the sensor element in the overall system (8:9).

1.1.3 MRTD Shortcomings When compared to measured values, the predicted MRTD obtained using the NVL model is optimistic (low) at low spatial frequencies and pessimistic (high) at high spatial frequencies (11:32). A number of

researchers have been working on an improved eye/brain model to reduce the discrepancy between measured and predicted MRTD in parallel scan thermal viewing systems. Hepfer (9) and Vortman (10:495) present papers which describe modified eye/brain spatial filtering techniques which correct for much of the observed discrepancies, however, these models cannot, without modification, adequately describe the performance of staring arrays. Also, it should be noted that MRTD is often associated with 'static' performance models where search and acquisition are not considered. A 'dynamic' model would probably be more appropriate for many military applications. In addition, there are serious problems associated with the use of MRTD as a figure of merit for second generation thermal imaging systems. Second generation systems typically employ staring and scanning focal plane arrays which introduce new parameters that MRTD fails to address. McCracken (11:32) presents some problems with the use of MRTD in evaluating thermal imaging systems. Sampling effects, non-uniform response, and scanning techniques are some of the parameters not addressed in many MRTD models. Also, the subjective nature of MRTD makes it ill-suited for use with automated test equipment (ATE) and automatic target recognition (ATR) algorithms. Currently, a number of researchers in the infrared community are looking for solutions to these problems.

1.2 Problem Statement

Presently, researchers do not agree on an optimal set of merit figures for assessing the performance of thermal imaging systems which employ staring focal plane arrays. Consequently, a generic focal plane array model is required to specify the relationships among the many parameters which contribute to overall FPA system performance. The model should establish and integrate a set of merit figures that may be used by system designers and program managers to more adequately specify FPA system performance requirements and more accurately predict system performance. Specifically, I will address the following research question:

How can one adequately include the effects of sampling and detector response nonuniformity into system performance modeling relations?

1.3 Scope

I will identify, compare, and contrast existing models for staring focal plane array systems. The model performance predictions will be compared against experimental data obtained in the laboratory. The most promising models will be examined further for possible extension and improvements. In doing so, I hope to establish, in the most general terms, the relationships among the critical FPA parameters affecting IR Imaging system performance. As an aid in evaluating the proposed merit figure(s), I will follow the guidance provided in the next section. Because of the Air Force interest in monolithic silicon technology (Platinum Silicide FPAs), I will look closely at PtSi Schottky-barrier technology. I will present guidelines regarding the specification, test, and evaluation of staring FPAs used in thermal imaging systems. Lastly, I will present the best modeling approaches for follow-on research.

1.4 Standards

The three primary applications for figures of merit are in controlling production quality, establishing manufacturer's typical performance specifications, and comparing different approaches prior to system design (12:30). I am primarily interested in presenting a figure of merit which can be applied to the last item and beyond perhaps; namely, system design. According to Humphreys (12:30), a good figure of merit (FOM) must fulfill the following requirements:

1. The FOM must provide an accurate measure of system performance.
2. The test conditions must be 'simple' and reproducible.
3. The FOM must apply to all functionally equivalent devices.
4. All parameters of the FOM must be measured, not inferred.

5. The FOM must provide unambiguous results.

In addition to the above requirements, the model should enable the system designer to make accurate performance predictions. The above criteria and the 'research questions' in the problem statement will be used as guidance in selecting the most appropriate FPA merit figures.

1.5 General Approach

Because I will identify proposed staring array models or extend existing first generation models, my research requires a sound understanding of existing TIS models and second generation system features. A thorough literature search will be performed using both the paper indexes and the available computer search services. This research will also require consultations with experts in the field. The knowledge gained by comparing the model predictions against measured MRTD values will be used to establish objectives for further research.

1.6 Thesis Organization

This chapter has provided a brief perspective on thermal imaging system modeling, introduced the MRTD concept, outlined the scope and objectives of the research effort, and identified the basic approach that will be used to accomplish the research goals. The next chapter will provide background on FPA modeling and Chapter Three will provide more information on the most promising system models. Chapter Four compares model predictions with experimental data for three different PtSi staring array cameras. Chapter Five presents conclusions and recommendations.

II. Relevant Background

2.1 Introduction

In the last chapter, the groundwork was presented for understanding TIS modeling. This chapter presents background material needed to understand basic Focal Plane Array technology, the linear systems theory commonly used to characterize optical systems, and how this theory applies to modeling Focal Plane Arrays. Lastly, a number of staring array models are introduced along with a discussion of how they might be improved.

2.2 Focal Plane Arrays

Focal Plane Arrays (FPAs) are electro-optical devices which convert spatial radiant energy (infrared) into temporal electrical signals. They generally take the form of large one or two dimensional arrays of detectors. The two dimensional arrays are often called mosaic detectors. A primary objective of Focal Plane Array technology is to exploit the advances in solid state technology by using an integrated circuit approach for detection in thermal imaging (13:183). A major advantage in this approach is the higher detector density on the focal plane and the improved sensitivity resulting from longer photon flux integration times. When used as part of thermal imagers, FPAs sense small changes in radiance caused by local apparent temperature differences. The term 'apparent' is used because differences in emissivity across a constant temperature surface also cause scene contrast.

2.2.1 Scanning Techniques Focal plane arrays are either mechanically or electrically scanned. Mechanically scanned FPAs rely on a rotating or oscillating mirror to scan the scene across a linear or one-dimensional array of detectors. The use of a conventional (mechanical) scan mechanism causes the systems using these FPAs to be larger, bulkier, and generally less reliable. The use of a mechanically scanned FPAs,

however, can lessen the effects of aliasing in the scan direction through oversampling and in the cross-scan direction by overlapping (interlaced) scan. Here, oversampling implies a sampling rate which exceeds the Nyquist limit. Also, scanning FPAs are able to take advantage of an on-focal-plane signal processing technique, time-delay and integration (TDI). The use of TDI increases the signal to noise ratio (SNR) in TDI arrays over those employing simple parallel scanning techniques. Electrically scanned or staring FPAs use a larger number of detector elements, ordered in a two-dimensional mosaic pattern, upon which the whole image is projected. Since, for each static scene, the detectors in the array constantly 'stare' at a portion of the scene within a frame time, the detector elements of the staring focal plane array are able to integrate the photon flux longer, thereby increasing overall sensitivity. This increased sensitivity can be seen to arise from long integration periods (33 milliseconds) for 30 Hz frame rates. This is especially important for low light level detection requirements, such as those specified for early warning systems.

2.2.2 FPA Fabrication FPAs are either monolithic or hybrid. These terms describe how they are fabricated. In the mid to far infrared, monolithic FPAs generally use a silicon substrate with detector elements consisting of narrow band gap extrinsic silicon. The detection and readout devices are fabricated in the same material; hence, the term monolithic applies. Another promising silicon monolithic FPA technology employs the internal photo-emissive effect. Here, a Schottky-barrier diode injects photo-generated current into a silicon substrate. Hybrid FPAs rely on coupling an IR sensitive material (narrow band gap semi-conductor such as mercury-cadmium-telluride HgCdTe) to a silicon substrate. An advantage of the hybrid approach is that the detector function can be optimized independently of the silicon readout device. A major disadvantage for large arrays is the difficulty in reliably interconnecting the detector material to the substrate. This reduces yield and increases overall system cost.

2.3 *Linear Systems*

Linear systems theory is commonly used to assess the performance of imaging systems by describing the system's response to different spatial frequencies. The frequency response of a linear-shift-invariant (LSI) optical system is often called the Optical Transfer Function (OTF). Since the OTF is a complex number, the modulus of the OTF is often used instead and it is known as the modulation transfer function (MTF). Gaskill (14) and Goodman (15) provide excellent introductory treatments of linear system applications in optics.

2.3.1 Sampled Imaging Systems Linear system theory, however, must be applied carefully to sampled imaging systems. For the MTF to be meaningful as a system description, the system should be an LSI system. Since sampling is neither linear nor shift-invariant, special care must be taken when applying linear systems theory to sampled imaging systems.

2.3.2 Isoplanarity Shift-invariance is a one-dimensional, temporal concept. For spatial systems, the term isoplanarity is used to indicate space-invariance. Thus, an imaging system is isoplanatic if, as the object is moved in the object field, the image remains the same in form (not location) in the image field (15:19). Sampled imaging systems are not, in general, isoplanatic. Small changes in the location of periodic objects can produce dramatic changes in the sampled image output. An example which dramatizes this point is imaging a checkerboard pattern. If the array detector elements are ordered similarly, one can imagine how the array elements might all have footprints on the white squares, which would be interpreted as a bright, uniform background. On the other hand, a small change in the checkerboard pattern location could cause all the black squares to be imaged, implying a totally different (darker) scene.

2.3.3 Aliasing The early work of Whittaker and Shannon was originally applied to one dimensional sampling in data communication applications (15:21). Fortunately, the extension to two dimensional sampling is relatively straight forward. For a band-limited signal to be reconstructed completely, it must be sampled at twice the highest occurring frequency. However, since the sampling rate at the focal plane (for staring arrays) is fixed by the detector spacing (pitch), any spatial frequencies $f > 1/2p$ where p is the detector pitch will be aliased onto the image spectra. The aliasing is a sum and difference heterodyne type effect and introduces artifacts and moiré patterns in the resulting imagery. For non-periodic scenes, the effects are unpredictable, and therefore, very difficult to model.

2.4 FPA Modeling

TIS models generally consist of three rather distinct elements; these include the target signature/background model, the atmospheric model, and the imaging system model (8:2). This report examines imaging system modeling only. More specifically, this report is concerned with the use of staring FPAs in TI sensor systems. The major FPA modeling elements, which can be analyzed separately, are presented below:

1. The detector array sampling effects.
 - Detector geometry, e.g., square, ovoid, *etc.*
 - Array lattice, e.g., hexagonal, rectangular, *etc.*
 - Scanning techniques, e.g., staring, microscanning, *etc.*
2. The detector response (quantum efficiency and noise level).
3. Transfer and readout techniques.
4. Response nonuniformity.

Recent work in these major areas will be presented, some of the proposed figures of merit for FPAs will be discussed, and lastly, a number of MRTD models for staring array systems will be introduced.

2.4.1 Sampling Effects The finite detector size in FPAs result in a sampled image. Montgomery (17:700) discusses the effects of sampling on imaging systems and concludes that the usual discussions regarding the MTF of sampled systems are oversimplified. Wittenstein (18:41) also discusses sampling effects and extends the concept of the Optical Transfer Function to sampled systems. He does this by redefining isoplanarity, and presents a modified figure of merit for sampled imaging systems that requires a description of the residual aliasing present. Bradley (19:53) discusses the effects of sampling in HgCdTe FPAs and also investigates the non-isoplanatic nature of FPA systems. He recommends the use of microscanning as method of reducing the deleterious effects of sampling. Cox (20:62) and Mercereau (21:57) investigate the effects of using hexagonal lattices and detector elements and conclude that, for certain non-imaging applications, a hexagonal lattice is more efficient than the conventional rectangular lattice. Marshall (22:69) studies the effect on MRTD of various detector shapes and concludes that an elliptically shaped detector yields better performance than the traditional square shaped detectors.

2.4.2 Detector Response The primary detectors used in FPAs are photoconductive, photovoltaic, and Schottky-barrier detectors. The photovoltaic detector's influence on FPA performance is described by the charge diffusion model. Charge diffusion modeling accounts for the absorption of incident photons, conversion of the photons to charge carriers, and the diffusion, recombination, and collection of signal current. Seib (23:210) discusses charge diffusion effects on the MTF of charge coupled imagers and presents results that could possibly be extended to monolithic extrinsic silicon FPAs. More recently, Thurlow (24:2) discusses charge carrier diffusion modeling (CCDM) as a tool for evaluating FPA performance by characterizing

important parameters such as spectral response, noise equivalent irradiance, and MTF.

2.4.3 Transfer and Readout Once photo-generated electrons are created, they need to be transported off the FPA. The two most common readout mechanisms are those employing charge coupled devices (CCDs) and charge injection devices (CIDs). Of these, the use of CCDs is most common. The CCD is basically a string of Metal Oxide Semiconductor (MOS) capacitors which function as an analog shift register. The CCD has found its way into many applications; these include their use in CCD memories, analog signal processing devices, as well as in solid state imaging arrays. Amelio was the first to publish the results of a CCD computer model in 1972 (24:250). Barbe presented a classic paper on CCD imaging in 1975 (25:63). He calculates the Modulation Transfer Function (MTF) for both front and back illuminated CCD imagers. Although his paper is primarily a discussion on visible CCD imaging, his general approach and some of his results transfer directly to the problem of modeling FPAs employing a CCD readout. Barbe identified three factors affecting the MTF of CCD imaging systems. They include the cell geometry (size, shape and center-to-center spacing of detectors), charge diffusion between photon conversion and photo-electron collection, and charge transfer efficiency (CTE). Although Barbe presents a very thorough analysis of charge transfer inefficiencies and their effect on the CCD MTF, the treatment regarding cell geometry and charge diffusion is not as complete.

2.4.4 Response Nonuniformity Response nonuniformity of detectors in an array seriously limit the performance of staring FPA systems. These nonuniformities result from the combination of responsivity variations in the detector, imperfect coupling, and fabrication tolerances. Because of the low contrast in thermal imagery, it is important to control the spatial noise introduced by these nonuniformities. Since this noise is spatial (fixed pattern) and not temporal, it cannot be removed

through frame averaging. In some cases, the serious effects of nonuniformity may be corrected with appropriate processing. Mooney and Deraniak (26:223) show how response nonuniformity impacts TI system design. For photon-noise limited performance, nonuniformities must be less than .01% (27:18). This is beyond what present photolithography processes can accomplish. Milton *et al.* (27:855) describe some correction techniques for both linear and non-linear nonuniformities and present a method for predicting the sensor Noise Equivalent Temperature Difference ($NE\Delta T$) before and after nonuniformity correction. $NE\Delta T$ is the large target temperature difference required to produce a signal to noise (SNR) equal to one at the output of a reference filter.

2.4.4.1 Characterization The effects of response nonuniformity must be adequately characterized before existing models can be modified to account for the performance degradation caused by fixed pattern noise. Marguia and Ewing (28:121) present a statistical model for characterizing the noise contribution: the result is a variance of the pixel nonuniformity. Boreman (29:988) feels that too much information is lost by describing the noise simply by the variance. He advocates a characterization in the Fourier domain to better describe the "nonwhite" nature of the noise spectrum. Mooney *et al.* (30) introduce a new figure of merit, the Contrast Signal to Noise Ratio (CSNR), which reduces to $1/NE\Delta T$ when no spatial noise is present.

2.4.4.2 Compensation Compensation of nonuniformity can be accomplished by irradiating the array with a uniform field and computing correction factors. This can be done at a number of irradiance levels, where a N-point fit indicates N calibrated irradiance levels and N sets of correction factors. As one might expect, the approximation improves with larger N. In principle, the correction could be accomplished to arbitrary precision, but Mooney *et al.* (30) show that spectral variations in responsivity establish fundamental limits on the accuracy of correction

techniques. The relation between quantum efficiency and fixed pattern noise established by Mooney *et al.* reinforces the need for characterizing response uniformity in TIS models.

2.5 FPA Figures of Merit

Several papers touting modified FPA figures of merit and a few actual FPA models have been presented in various technical journals. Mooney and Deraniak (26:223) show that spatial noise caused by detector response nonuniformity argue for using signal to noise as the preferred figure of merit. Humphreys (12:35) defines a figure of merit for a staring FPA that reduces to the detector D^* for a one element array. Effects of nonuniformity are not included. Cross and Reese (31:195) present five figures of merit which apply to FPA sensors—transfer characteristics, spatial response, spectral response, uniformity of response, and image retention. Deraniak (32:256) believes no single figure of merit is capable of describing the performance of FPAs. This seems reasonable considering the enormous complexity of today's advanced detector arrays. He recommends five measures—filling efficiency (ratio of photoactive to inactive area on array), spatial resolution, modulation transfer function, quantum efficiency, and integration time (or bandwidth). Without a model to tie these five merit figures together, however, it is difficult to perform the tradeoffs required during system design. A number of researchers simply advocate modifying the existing MRTD models by adding noise and MTF expressions appropriate for the particular FPA (8, 33). The computer model described by Thevdt *et al.* (34:256) looks at FPA sensitivity, spatial charge movement, and MTF for a variety of detector materials using several different read-out techniques. However, since the model only considers the zero frequency MTF, it would have to be extended to other spatial frequencies to obtain a useful MRTD model.

2.6 Improved MRTD Models

In spite of its drawbacks, MRTD is really the best summary measure we now have for evaluating thermal imaging systems (35). A great deal of effort has been spent on validating MRTD models and the correlation with field performance is not bad (within 20%) (36:4). Improvements to MRTD models may be the best approach to satisfying the research objectives in Section 1.2.

2.6.1 Second Generation Effects Presently, many MRTD models do not address MTF degradation in the cross-scan direction due to undersampling. When undersampling does occur, as in staring arrays, the effects on image quality are not well understood. Large detector arrays, staring and scanning, are plagued by non-uniformity effects which also are not addressed by some MRTD models.

2.6.2 Objective Standard There are significant misgivings concerning the subjective nature of MRTD. Not only would an objective measure make standardization easier, it would help integrate Automatic Test Equipment requirements into the design process. Currently, work is underway to develop techniques for *objectively* measuring a thermal imaging system's MRTD (6, 7, 16). As mentioned earlier, MRTD is a figure of merit that accounts for both the sensitivity and resolution of the TI system. Sensitivity depends upon system noise, and the system noise is described by a number of quantities; these include Noise Equivalent Power (NEP), Noise Equivalent Irradiance (NEI), and Noise Equivalent Temperature Difference ($NE\Delta T$) (8:9). The system resolution is described by its Modulation Transfer Function (MTF). The system noise and resolution measures combine to yield MRTD (8:9). Since the system's MTF and $NE\Delta T$ can be measured directly or calculated theoretically, modeling the system's MRTD presumably reduces to a problem of more manageable size; namely, modeling the system noise figure ($NE\Delta T$) and resolution figure (MTF). However, as we will see, even with perfect knowledge of the array $NE\Delta T$ and MTF, the functional relations existing between them to form MRTD can be many and varied. The source

of much of the difference in various MRTD expressions can be traced to differing assumptions regarding the eye/brain spatial filtering function.

2.7 Staring Array MRTD Models

This research has uncovered six candidate staring IR System MRTD models. Three of the models are modified versions of the NVLSPM; they include the Battelle Middle Wave Infrared (MWIR) Sensor Model (37), the MICOM Infrared Imaging Sensor Performance Model (MIISPM) (8), and Martin Marietta's Model (MMM) presented by Contini and Honzik (33). The other three include the RCA model presented by Cantella (38), the Psychophysical Periodic Model (PPM) for Platinum Silicide (PtSi) Staring Arrays presented by Rosell (39), and the two-dimensional MRTD model presented by Kennedy of Texas Instruments (40). Table 2-1 summarizes some general information concerning the above staring array models. General discussions regarding the eye/brain filtering functions, aliasing and nonuniformity treatments are found in the following subsections. Detailed discussions concerning the MWIR, Kennedy and Rosell model are found in Chapter Three.

2.7.1 Eye/Brain Models Since the early days of television, extensive research has been conducted on the perception of information displayed on television type monitors. The eye/brain, much like any radiation detector, is subject to random fluctuations in signal and is plagued by internal noise which interferes with the detection process. De Vries (1943) postulated and Rose (1948) verified that an image must have a SNR exceeding a threshold value for detection to take place (5:169).

The hypothesis suggested by this is that the visual system establishes a signal-to-noise ratio threshold as a reference to test for the significance of neural impulses. The effect is that low SNR optical signals are not detectable, but also that low level noise events are not mistaken for signals. Thus we are not constantly mentally disturbed by fleeting impressions (false alarms) of objects which do not exist. (4:147)

Staring Array Model	MTF Expression Defined	Eye/Brain Spatial Filter	Aliasing Treatment?	Nonuniformity Treatment?
MIISPM	partial	matched filter	yes	no
MWIR	yes	matched filter	no	yes
MMM	yes	matched filter	no	yes
RCA	no	synchronous integrator	no	yes
Rosell	yes	synchronous integrator	no	yes
Kennedy	no	hybrid matched filter	yes	no

Table 2.1. Staring Array Models

Psychophysical research has shown that, for a given target SNR, the larger the angle subtended by the target at the eye, the easier it will be to detect. This suggests a spatial filtering process in the eye/brain which improves the perceived SNR (SNR_p) over that of the displayed SNR (SNR_d). The matched filter and synchronous integrator models are analytic attempts to model the complex spatial filtering performed by the human observer. Also, experiments have shown that the eye/brain sums and stores signals slightly separated in time. Assuming the noise from frame to frame is uncorrelated, the eye/brain sums the signal directly while the noise is represented by its root-mean-square value. This results in a SNR enhancement proportional to the square root of number of independent frames within the eye integration time (4:132). Given a frame rate F_R of 30 per second and an eye integration time t_E of .1 seconds, the SNR enhancement factor would be equal to $(t_E F_R)^{1/2}$ or $\sqrt{3}$. Many of the differences in the above models can be traced to the different spatial and temporal enhancement factors assumed.

2.7.2 Aliasing The effects of sampling, particularly aliasing, are often ignored in MRTD models. Of the six models above, only the MICOM and Kennedy modeling attempt to handle aliasing.

2.7.2.1 MRTD Range MRTD measurements using staring array sensors indicate that the bars cannot be resolved, at any temperature, much beyond half the nyquist frequency. Assuming it takes a minimum of seven samples to represent a four-bar pattern, the maximum spatial frequency where four bars can be individually resolved is $.57f_{smp}$ or $\frac{4}{7}f_{smp}$ where $f_{smp} = 1/p$ and p is the detector pitch in the direction across the bar pattern (41:100). At spatial frequencies beyond $.57f_{smp}$ the MRTD is essentially infinite; therefore it would serve no purpose and is somewhat misleading to present values of MRTD beyond this point.

2.7.2.2 Phase Dependence For periodic targets, sampling effects depend a great deal upon the phase between the target and focal plane array sampling lattice. This phase dependence is most dramatic when the spatial frequency of the target approaches f_{nyq} or $.5f_{smp}$. At or near f_{nyq} , the aliased components can either enhance or diminish the wanted signal. A common procedure followed in the laboratory for measuring MRTD at or near f_{nyq} is to align the bar target for maximum response. In this manner, the sampling phase becomes a condition of the measurement.

2.7.2.3 Aliasing and Imagery The above subsections provide a first order treatment of aliasing but it does not describe the effect of aliasing on the imagery. As mentioned earlier, aliasing occurs when the target spatial frequencies are under-sampled. This results in the folding (about f_{nyq}) of the target spectra onto lower spatial frequencies. Kennedy (40:120) suggests an approach for aperiodic targets whereby the spectral energy in the scene above f_{nyq} (as filtered by the system response) is treated as an additive white noise source. The MICOM model follows Kennedy's lead in this regard but goes on to define a separate $NE\Delta T$ due to aliasing. In both models, the implication for MRTD is that as the frequency content of the bar target approaches f_{nyq} , the amount of noise due to aliasing increases. This results in a correction term to the MRTD which is very small at first but grows rapidly as the spatial frequencies exceed f_{nyq} . However, we will see that, since most of the models overpredict (predict high MRTD) at higher spatial frequencies, the need for this correction becomes moot.

2.7.3 Nonuniformity Treatment All the models discussed above treat nonuniformity except the MICOM model and the Kennedy model. However, since the general approach followed by the other four models is to incorporate the nonuniformity into the $NE\Delta T$ expression, the Kennedy and MICOM models could be extended in a similar manner. Cantella (38) first suggested that noise sources should be classified

according to their functional relationship to background exposure. Depending upon background radiance and relevant system parameters, any one of these noise classes can dominate. The classes are as follows:

- Quantum
- Multiplicative
- Additive

Quantum noise sources are proportional to the square-root of the background exposure (photon noise). Multiplicative noise varies proportionally to the background (fixed pattern). Additive noise (dark current shot noise) has no dependence on background exposure. Fixed pattern noise cannot be removed through frame averaging the way temporal noise can. Cantella and those that followed have characterized the fixed pattern noise in the array as an rms deviation from some mean value. This is also consistent with the CSNR defined by Mooney et. al (30).

2.7.4 A Closer Look The next chapter will describe in more detail the models presented by Battelle (MWIR), Rosell, and Kennedy. Of the three NVL type models, only the MWIR model will be described further. One reason is the extensive documentation which accompanies this model. Another reason is that there is evidence (10) that suggests the matched filter approach is not as good as the synchronous integrator model in describing the eye/brain behavior. Only one matched filter model is needed to test this hypothesis. The RCA model is very similar to the Rosell model except the RCA model describes noise in terms of electrons per pixel whereas the Rosell model uses noise current. The last model which will be considered is the Kennedy model. Since his approach is unique (it combines aspects of both the Rosell and MWIR) and his model addresses aliasing, further examination of the Kennedy model is warranted.

2.8 Summary

This chapter discussed basic focal plane array technology, introduced some linear systems concepts, addressed their use in describing sampled imaging systems, outlined FPA modeling areas, presented some recent work on FPA performance modeling, and identified MRTD as a promising kernel upon which to build further. Further, a number of staring FPA models were introduced, and their major differences and similarities were highlighted. The next chapter will outline the basic steps in MRTD derivations, and describe in greater detail the MWIR, Rosell and the Kennedy models.

III. Staring Array System Modeling

3.1 Introduction

This chapter looks at the MRTD modeling methodology and further examines the three staring FPA system models discussed earlier; these are the MWIR, Rosell and Kennedy models.

3.2 Modeling Methodology

3.2.1 MRTD Functional Form The TIS and eye/brain combination are modeled through the MRTD. As mentioned earlier, MRTD combines both the signal transfer characteristics represented by the MTF (system and eye) and the noise characteristics specified by the NE Δ T. The functional form of MRTD can be arrived at heuristically. Higher system sensitivity (lower NE Δ T) should allow smaller detectable temperature differences for a given spatial frequency, therefore MRTD should be proportional to NE Δ T. At higher spatial frequencies, the signal response is reduced due to MTF degradation, therefore stronger signals (larger temperature differences) will be required for small MTF values (higher spatial frequencies). As will be seen shortly, the functional form for MRTD can be expressed as follows:

$$\text{MRTD} \propto \frac{\text{NE}\Delta\text{T}}{\text{MTF}}$$

As implied by the above relation, modeling the staring array system MRTD requires knowledge of the array NE Δ T and MTF, and as we'll see, some basic assumptions regarding the eye/brain contribution.

3.2.2 Modeling Process Regardless of the model, four basic steps can be found within the modeling framework. Figure 3.1 illustrates the four step process involved in modeling MRTD. MRTD derivations typically begin with a description

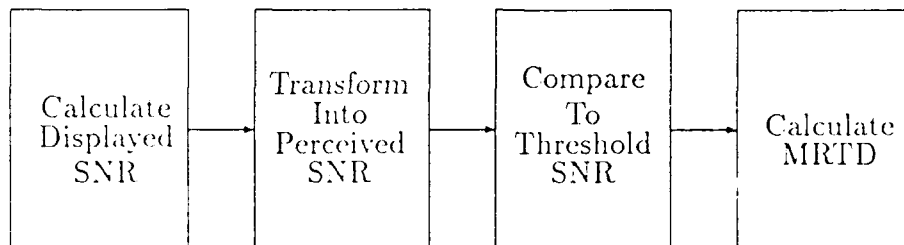


Figure 3.1. MRTD Modeling Process

of the target. This description includes the ΔT with respect to the background and its spatial frequency (for bar targets). The background is assumed to be a blackbody with constant temperature (no clutter usually is assumed). The target and background signal undergo radiometric transformations to arrive at a video or display signal to noise ratio SNR_d . The SNR_d is then transformed into a perceived SNR_p by means of spatial filtering and temporal integration. If $SNR_p < SNR_{th}$, then the target cannot be resolved. The temperature difference which yields a $SNR_p = SNR_{th}$ is the minimum resolvable temperature difference for that spatial frequency.

3.2.3 Sensitivity Analysis The differences in $NE\Delta T$ derivations are more a matter of style and preference than substance. However, an approach that proves very convenient for characterizing large arrays is to characterize the noise in terms of its variance (root-mean-square value per pixel). This rms value is generally given in units such as noise electrons/pixel or noise current/pixel. Treating the noise in this way not only makes it much easier to incorporate nonuniformity effects, it also allows application of the model in any spectral region (38:41). Section 3.4.2 outlines the manner in which nonuniformity is incorporated in the Rosell $NE\Delta T$ model.

<i>Component</i>	<i>MTF Expression</i>
Optics(15:120) (Diffraction Limited)	$\frac{2}{\pi} \left[\arccos \left[\frac{f}{f_c} \right] - \frac{f}{f_c} \left[1 - \left[\frac{f}{f_c} \right]^2 \right]^{1/2} \right]$ $f_c = \frac{1}{\lambda F \#}$
Detector Aperture(33:62)	$\frac{\sin(\pi \alpha f)}{\pi \alpha f}$ $\alpha = \text{detector IFOV}$
Electronics(39:183) Nth Order Butterworth	$\left[1 + \left[\frac{f}{f_{nyq}} \right]^{2N} \right]^{-1/2}$
Display(39:183)	$\exp^{- \left[\frac{f}{f_d} \right]^2}$ $f_d \text{ -flat field parameter}$

Table 3.1. Basic MTF Expressions

3.2.4 MTF Derivation The system MTF is an important parameter in the MRTD expression. Not only does it occur in the MRTD denominator, it also occurs (at least in part) within the noise filtering expressions in the numerator as will be seen shortly. Different models (both staring and scanning) not only use various MTF expressions, some models define MTF parameters not found elsewhere. Although this makes it difficult to establish a 'consensus' MTF expression, four elements are basic to all the models surveyed; optics, detector aperture, video electronics, and display. The functional forms for these MTF elements may be found in Table 3.1. The above expressions and inherent assumptions embodied by them are discussed in the following subsections. Also, other MTF terms not universally applied will be discussed further.

3.2.4.1 *Optics MTF* Often a correction consisting of a gaussian blur function is made for non-diffraction limited optics (43:8),(42:3- 1),(33:62). The correction becomes necessary to account for aberrations and defocus which are present in all systems to some degree. From a modeling perspective, it is very difficult to obtain this data. For the purpose of comparing model performance in Chapter Four, diffraction limited optics are assumed. Figure 3.2 includes the optical MTF for one of the cameras (Camera-One) used in the model comparison in Chapter Four. The other MTF curves shown in Figure 3.2 are discussed in the next few sections.

3.2.4.2 *Detector Aperture* The detector samples the scene, and since the size of the detector is finite (rather than an impulse), it performs a spatial filtering function (43:8). Assuming a uniform response over the detector active area, the detector transfer function is the 2D Fourier Transform of the detector shape. For rectangular detectors, this results in a $\sin(x)/x$ function in each direction as illustrated in Table 3.1. For scanning systems, it is the detector width which usually determines resolution. In contrast, the resolution of staring systems is limited by the detector spacing or pitch (44:269). In an attempt to model the sampling effects introduced by staring imagers (or the sampling effect in the cross-scan direction in parallel scan viewers) some models (33, 48, 42) introduce a MTF factor due to sampling of the form:

$$\text{MTF}_{\text{simp}}(f_x) = \frac{\sin(\pi \phi_x f_x)}{\pi \phi_x f_x}$$

where ϕ_x is the detector angular pitch in the horizontal (x) direction. The validity of this approach is in question and can be considered only a first order approximation of the sampling effect (45:97). Since sampling is not a linear process, attempts to model it by simply using a deterministic transfer function should be viewed with caution. A more precise and presumably more accurate approach is discussed in Section 3.5.2. Because of the long dwell times associated with staring imagers, the temporal response of the detector (essentially unity in passband) need not be

considered for static applications. Figure 3.2 shows the detector MTF for one of the cameras (Camera-One) used in the model comparison in Chapter Four.

3.2.4.3 Electronics MTF The electronics transfer function represents the contributions from a number of elements; these may include input circuit response, CCD transfer inefficiency effects, aperture correction (boost), multiplexer, preamplifier, uniformity correction, and video amplifier and filter (46:159). Obtaining parameters for these functions is difficult for available systems and projecting parameters for future systems would, again, be a matter of guesswork. For the purpose of comparing the various MRTD models, a second order butterworth filter is assumed with the poles at the nyquist frequency f_{nyq} . Although this is admittedly an oversimplification, it should not unduly bias the comparison results. It is also in agreement with the study by Vortman and Bar-Lev (47:135) which finds the optimum electronic response for sampled systems is a double pole filter at the nyquist frequency. Figure 3.2 illustrates the electronics MTF for one of the cameras (Camera-One) used in the model comparison in Chapter Four.

3.2.4.4 Display MTF The functional form for the display transfer function is gaussian with a spread determined by the factor f_d where f_d is chosen to yield a flat field condition. A flat field condition is achieved when the raster in the display is no longer discernable. Although this depends in part on the viewing distance, a flat field condition may be obtained when (48:219).

$$MTF_{dsp}(2f_{nyq}) \leq .005$$

This relation was used in modeling the display MTF for the model comparisons in Chapter Four. Figure 3.2 includes the display MTF for one of the cameras (Camera-One) used in the model comparison in Chapter Four.

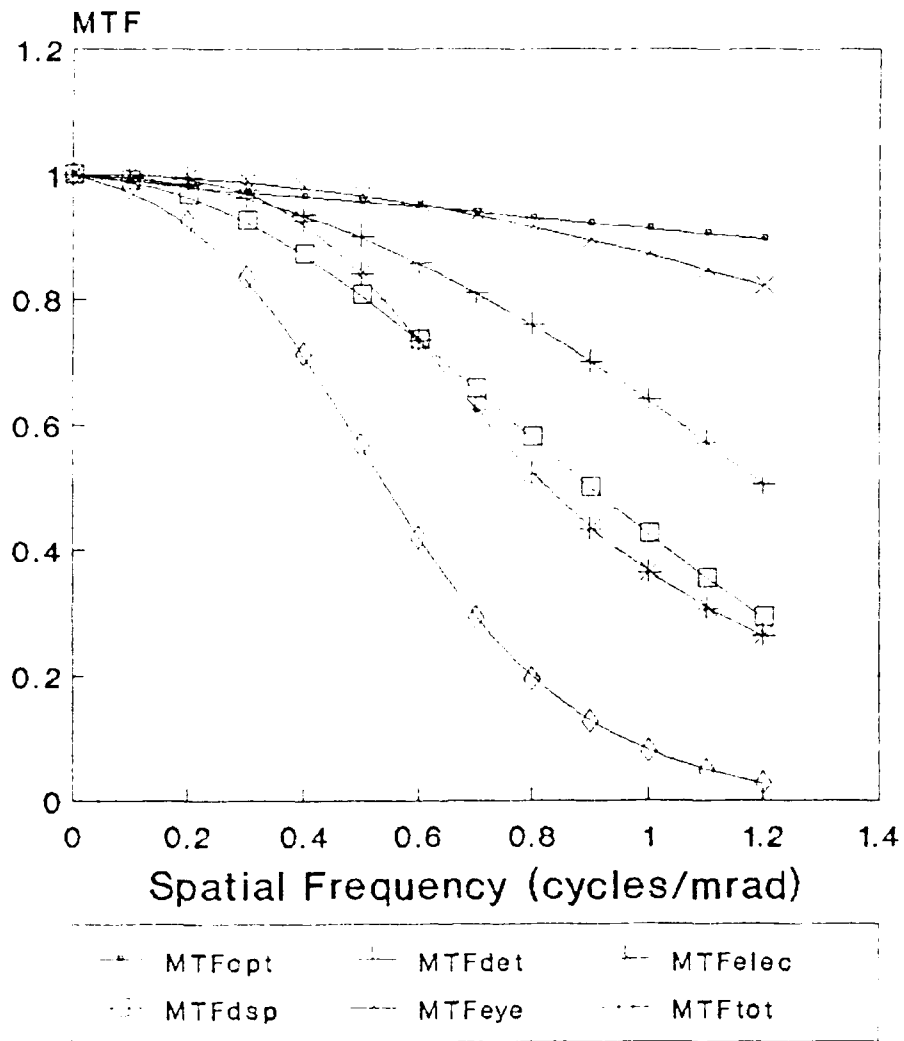


Figure 3.2. Typical Camera MTFs

3.2.4.5 *Eye MTF* A number of models employ a simplified version of the eye transfer function presented by Kornfeld and Lawson (49). These include the NVL, MWIR, Martin Marietta, and the MICOM models. In its simplified form the transfer function is a decaying exponential which decays at a rate determined by, Γ , a light-level dependent decay factor and M , the system magnification.

$$H_{eye}(f) = \exp^{-\Gamma f/M}$$

The eye MTF depends upon the light level because at higher light levels, the pupil becomes smaller. This stopping down of the eye aperture reduces the number of off-axis rays reaching the retina which, in turn, reduces the effect of aberrations in the eye lens. Hence, for higher light levels, the curve decays more slowly. Figure 3.2 includes, along with the other MTF curves, a typical eye MTF as a function of spatial frequency (cycles/milliradian). This model is an adequate description of the diffraction and aberration effects of the eye for spatial frequencies exceeding about .3 cycles/mrad (10, 4). "For lower spatial frequencies there is a decrease in response that cannot be attributed to the eye lens and must be related to some type of image processing done in the inner eye-brain system (10:494)." It is this decrease in response at low frequencies which causes some models to include a saturation term which limits the spatial integration at low frequencies. As mentioned earlier, the eye transfer function above is a simplified version of the excitation-inhibition model presented by Kornfeld and Lawson. In fact, the above expression is only the excitation portion of the model presented by Kornfeld. The inhibition portion forces the response function toward zero at lower spatial frequencies. NATO conducted a modeling exercise in which a number of member countries compared the results of their thermal imaging system models. All the member countries, save the U.S. (which used the NVL model), either employed the excitation-inhibition eye model or employed a low spatial frequency correction factor by limiting spatial integration in the low frequency range (50:37). It would appear wise to keep separate the

passive elements (diffraction and aberrations) which are easily described by transfer functions from the 'active' signal processing functions accomplished in the eye/brain subsystem. Since Kennedy (40) and Vortman (10) already account for the low spatial frequency behavior of the eye/brain, it wouldn't make sense (in those models) to include an eye MTF which attempts to do more or less the same thing. Moreover, all the models based on the NVL model ignore this inhibition term in modeling the eye MTF. The Rosell model doesn't even use an MTF for the eye. The exclusion of an eye MTF can be justified in part because the reduction in response is small (See Figure 3.2). Thermal imaging system magnification is chosen such that the eye response is not a limiting factor. Also, during MRTD measurements, the trained observer (conducting measurements) is allowed to move his head toward and away from the display, which tends to optimize his viewing position. As a practical matter, because of the lack of information regarding the display luminance and magnification for the cameras used in the model comparison, an eye MTF was not used in the model comparison in Chapter Four.

3.2.4.6 Other MTF Contributions A number of MTF parameters have been introduced to account for factors such as line of site jitter (vibration), atmosphere, and overexposure (8:10). Vibration and atmosphere can usually be ignored in laboratory measurements and will not be included in the model comparison. The overexposure MTF was introduced by Borg (8) to describe the effect of transferring charge off the array while the array is still exposed to the scene. Assuming the transfer is rapid, usually a good assumption, this effect is small and also will be ignored in the model comparison.

3.2.5 Temporal Integration The eye/brain combination performs temporal noise filtering which is approximated by a fixed integration time, t_E , which is not precisely known, but is generally held to be between .1-.2 seconds (4:133). There is also some evidence that the integration time is not fixed but varies with light level,

but this is generally ignored in most models (4:132). This integration improves the perceived SNR by a factor of $(t_E F_R)^{1/2}$, where F_R is the frame rate.

3.2.6 Spatial Integration The eye/brain combination also performs narrow band spatial filtering which may be described by either one of two submodels: an adaptive matched filter model or a synchronous integrator model (10:492).

3.2.6.1 Adaptive Matched Filtering This submodel models the spatial integration performed by the eye/brain as a postulated matched filter having the same spatial frequency content as the bar target. A matched filter is a filter which maximizes the SNR. Although matched filtering isn't the actual physical process performed by the eye/brain, it does provide reasonably good agreement with perception test data. In order to resolve four bars, it is often assumed that at least one bar must be resolved. Therefore, the representation of the matched filter in the spatial frequency domain is the two-dimensional Fourier Transform of a single bar. The assumption inherent in the above discussion is that the image detection takes place in the presence of white noise. Since the image is sampled after the lens aperture, and because of the filtering function of the lens, the distribution of the noise is not white. Failure to account for the non-white nature of the noise leads to the choice of a filter which fails to maximize the SNR (10:494).

3.2.6.2 Synchronous Integrator Model Originally proposed by Schade, the synchronous integrator model has been used for years to evaluate television and other electro-optical systems. This theory actually predates the matched filter concept by 15-20 years (48:181). The model views the eye/brain as "an area integrator synchronized to the perturbation inserted by the target edges (10:498)." The eye/brain integrates signal and noise over an angular region defined by the target shape as it is modified by the system response. Another way of looking at this model is in terms of noise equivalent apertures. It can be shown using basic Fourier

relations that the energy in an optical signal is spread but not lost through optical apertures (assuming no dissipation) (5:176). Apertures (here the term really implies any MTF or transfer function) have been shown to decrease the SNR of signals. Since the signal energy is unaffected by the aperture, the conclusion is that apertures increase noise. Since the image area is larger, and photodetection is a noisy process, the increased noise from apertures is due to the integration of the signal over a larger (noisy) area.

3.2.7 Threshold The eye/brain combination requires a certain SNR to be able to perform detection and recognition tasks. The threshold SNR is an empirically derived constant and is expressed as SNR_{th} to emphasize *threshold*. The term *constant* is used loosely here because at lower spatial frequencies, it tends higher and at higher spatial frequencies, it tends to be lower. The general approach is to assume a constant threshold and make appropriate empirical curve fitting corrections at the extreme spatial frequency ranges. The NVL and MWIR models use 2.25 as the nominal SNR_{th} value. The Kennedy and Rosell models are silent on this point: a conversation with Rosell indicated anywhere from 2-2.5 was fine depending on how optimistic one wanted to be. The Rosell model, however assumes a t_E of .1 seconds as opposed to .2 for the NVL and MWIR models. This is in agreement with studies by Schade and others (4:132) and will be used for all model comparisons.

3.3 MWIR-Modified NVL Model

The most common model used for first generation thermal imaging systems is the Night Vision Laboratory Static Performance model, or NVL model (46:155). The popularity of this model is due in part to the extensive field performance validation that has been accomplished over the years. The limitations of the model are well known; the model ignores sampling effects in the cross-scan direction, provides optimistic results at low spatial frequencies and pessimistic ones at high spatial frequencies, and it is unable to handle staring systems where aliasing occurs in both

directions (36:4).

3.3.1 NVL MRTD There are a number of equivalent forms for MRTD. Below is the most general form used by the NVL model to describe parallel scanned thermal viewing systems. It is expressed as a function of spatial frequency along the scan direction (43:53):

$$\text{MRTD}(f_x) = \frac{\pi^2 \text{SNR}_{th} \text{NE}\Delta T}{8 \text{MTF}(f_x) L \int_{-\infty}^{\infty} H_L^2 H_D^2 df_y} \times \left[\frac{\Delta y v}{\Delta f_n F_R t_E} \int_{-\infty}^{\infty} \int_0^{\infty} \frac{S(f_x)}{S(f_{ox})} H_E^2 H_d^2 H_W^2 H_L^2 H_D^2 df_x df_y \right]^{1/2} \quad (3.1)$$

where

- SNR_{th} = required SNR to recognize bars
- Δy = vertical IFOV in milliradians
- v = detector scan velocity in mr/s
- f_x = target frequency in cycles per mr
- F_R = frame rate per second
- t_E = eye integration time
- Δf_n = electrical bandwidth
- $H_L(f_x)$ = electronic noise filtering function
- $S(f_x)$ = system noise power spectrum referenced to detector
- $S(f_{ox})$ = detector noise power spectrum at bar frequency
- $H_d(f_x)$ = display transfer function
- $H_W(f_x)$ = target filter function of bar-width W
- $H_L(f_x)$ = target filter function of bar-length L
- $H_D(f_x)$ = noise filter function from detector to display
- L = Bar Length (mrad)

and $NE\Delta T$ is given by

$$NE\Delta T = \frac{4F^2(\Delta f_n)^{1/2}}{\pi(N A_d)^{1/2}\tau_a\tau_o \int_{\Delta\lambda} D_\lambda^* W'_\lambda d\lambda} \quad (3.2)$$

where

- F = F-number
- A_d = detector area
- τ_a = average atmospheric transmission
- τ_o = optics transmission
- D_λ^* = detector specific detectivity
- N = number of detectors in series (if TDI used)
- W'_λ = temperature derivative of Planck blackbody equation
- $\Delta\lambda$ = spectral band of interest

3.3.2 Simpler Forms Although the MRTD relation given in Equation 3.1 is the most general form, a more useful form may be found by making the following substitutions (43:54):

$$q_v \equiv L \int_{-\infty}^{\infty} H_L^2 H_D^2 df_v$$

$$\rho_x \equiv 2W \int_0^{\infty} \frac{S(f_x)}{S(f_{ox})} H_E^2 H_d^2(f_x) H_W^2 df_x$$

$$\rho_v \equiv L \int_{-\infty}^{\infty} H_L^2 H_D^2 H_d^2(f_v) df_v$$

$$L = \frac{7}{2f_x}$$

$$W = \frac{1}{2f_x}$$

The quantities L and W are the angles in milliradians subtended by the bar length and width respectively. Using the above relations, the expression for MRTD reduces to (43:54)

$$\text{MRTD} = \frac{\pi^2}{8} \frac{\text{SNR}_{th}}{\text{MTF}(f_x)} \frac{\text{NE}\Delta T}{q_y} \left(\frac{\Delta y_i v}{F_{RtE} \Delta f_n} \frac{7}{2} f_x^2 \rho_x \rho_y \right)^{1/2} \quad (3.3)$$

Since the bar length is long compared to the system response, *i. e.*, the transfer function of matched filter is narrow compared to system response function, the quantities q_y and ρ_y will be approximately equal to one. With this assumption, the above MRT expression reduces to (43:54)

$$\text{MRTD} = \frac{\pi^2}{4\sqrt{14}} \frac{\text{SNR}_{th} \text{NE}\Delta T f_x}{\text{MTF}(f_x)} \left(\frac{\Delta y_i v \rho_x}{F_{RtE} \Delta f_n} \right)^{1/2} \quad (3.4)$$

Also Δy_i can be expressed

$$\Delta y_i = \frac{\Delta y}{\eta_{ovsc}}$$

Where Δy is the detector angular pitch in the vertical direction and η_{ovsc} is the over-scan ratio generally equal to one for staring systems. Finally, assuming $S(f_x)/S(f_{ox})$ equals one, *i. e.*, assuming white noise, ρ_x can be given by (43:56)

$$\rho_x = \frac{1}{(4f_x^2(\Delta x)^2 + 1)^{1/2}}$$

Using these two approximations yields the following expression which represents the MRTD form employed by the MWIR model (42:4-4):

$$\text{MRTD} = \frac{\pi^2}{4\sqrt{14}} \text{SNR}_D \frac{\text{NE}\Delta T f_x}{\text{MTF}(f_x)} \left(\frac{\Delta y V_s}{\eta_{ovsc} F_{RtE} \Delta f_n} \right)^{1/2} (4f_x^2(\Delta x)^2 + 1)^{-1/4} \quad (3.5)$$

For staring array systems, a few terms must be redefined. The term V_s is now the

equivalent scan velocity for the staring array defined by (42)

$$V_s = V H F_R \eta_{sc}$$

where V and H are the number of detectors in the vertical and horizontal directions, F_R is the frame rate, and η_{sc} is the scan efficiency. The noise bandwidth Δf_n is also redefined as follows (42):

$$\Delta f_n = \frac{V H F_R}{2}$$

It is the expression represented by Equation 3.5 which will be used to evaluate the predictive power of the MWIR model in the next chapter.

3.4 Rosell Model

The Rosell Model is a simplified version of the one presented by Sendall and Rosell in 1979 (48:200). These models are based upon the noise equivalent aperture theory introduced by Schade and discussed in Section 3.2.6.2. The basic formula is presented here with notation consistent with the MWIR model presented previously.

3.4.1 Rosell MRTD The following MRTD expression differs from the one presented by Rosell in that the term $NE\Delta T$ is explicitly represented here (39:185). The $NE\Delta T$ term is included in the expression below to emphasize the similarity in the models presented.

$$MRTD(f_x) = SNR_{th} \left[\frac{\gamma}{\epsilon t_E} \right]^{1/2} \frac{\pi^2}{4} \frac{f_x \varphi_v}{MTF(f_x)} NE\Delta T \left[\frac{\beta_N(f_x)}{2\Delta f_n} \right]^{1/2} \quad (3.6)$$

where

- SNR_{th} = required SNR to recognize bars
- γ = picture aspect ratio (H:V), typically 4/3
- ϵ = bar pattern length-to-width ration (7)

- t_E = eye integration time
- φ_v = vertical field of view (mrad)
- β_N = noise filtering function
- Δf_n = noise equivalent bandwidth

where

$$\Delta f_n = \frac{V H F_R}{2\eta_{sc}}$$

with V, H, F_R , and η_{sc} defined as before and the noise filtering function is given by

$$\beta_N(f) = \frac{1}{f} \int_0^f [H_E(f)H_d(f)]^2 df$$

where $H_E(f)$ and $H_d(f)$ represent the electronic and display transfer functions as before (39:184).

3.4.2 Rosell NE Δ T The NE Δ T derivation is presented to highlight the manner in which fixed pattern noise arising from response nonuniformity may be incorporated into MRTD expressions. This treatment is very similar to that found in the RCA and Martin Marietta models. A number of additional noise sources can easily be included but for the purpose of demonstration, only background, fixed pattern, and dark current noise are considered.

3.4.2.1 Calculating SNR_d The Responsivity of PtSi Schottky Barrier Diode devices is often represented by the modified Fowler equation (39:171)

$$R(\lambda) = C_e \left[1 - \frac{\varphi_{ms}\lambda}{1.24} \right]^2$$

in units of amps/watt where C_e is the quantum efficiency coefficient expressed in eV⁻¹ and φ_{ms} is the metal-semiconductor Schottky barrier expressed in eV. The

change in irradiance due to incremental changes in temperature is given by (39:172)

$$\Delta E(\lambda) = \frac{\tau_o(\lambda) \partial M(\lambda, T)}{4F^2 \partial T} \Delta T$$

where τ_o is the optical transmittance, F is the lens $F\#$, $M(\lambda, T)$ is the radiant exitance, and T is the background temperature K° . As long as $\exp^{C_2/\lambda T} \gg 1$, the temperature derivative of the radiant exitance can be given by (4:22)

$$\frac{\partial M(\lambda, T)}{\partial T} = \frac{C_1 C_2}{T^2 \lambda^6} \exp^{-C_2/\lambda T}$$

where C_1 and C_2 are the first and second radiation constants respectively. The incremental signal current Δi due to changes in temperature is given by (39:172)

$$\Delta i(\lambda) = \frac{\eta_{ff} A_{fp} R(\lambda) \Delta E(\lambda)}{\eta_{sc}}$$

where η_{ff} is the array fill factor, A_{fp} is the focal plane area, and η_{sc} is the scan efficiency. Substituting the expression for $\Delta E(\lambda)$ and integrating over the spectral band of interest yields (39:173)

$$\Delta i = \Delta T \left[\frac{\tau_o \eta_{ff} A_{fp} C_1 C_2 C_e}{4\eta_s F^2 T^2} \int_{\lambda_1}^{\lambda_2} \left[1 - \frac{\varphi_{ms} \lambda}{1.24} \right]^2 \frac{\exp^{-C_2/\lambda T}}{\lambda^6} d\lambda \right]$$

For a given spectral band and ambient temperature, the quantity in brackets is a constant and is denoted K_s , whereby

$$\Delta i = K_s \Delta T$$

Assuming unity optical transmission, the background current is given by (39:174)

$$i_b = \frac{\eta_{ff} A_{fp}}{4\eta_c F_c^2} \int_{\lambda_1}^{\lambda_2} R(\lambda) M(\lambda, T) d\lambda$$

where η_c and F_c are the cold shield efficiency and F# respectively. The blackbody exitance $M(\lambda, T)$ is given by

$$M(\lambda, T) = \frac{C_1}{\lambda^5} \exp^{-C_2/\lambda T}$$

The photon noise is given by

$$I_b^2 = 2qi_b\Delta f_n$$

where q is the electron charge and Δf_n is the noise equivalent bandwidth as defined before. Combining the above yields (39:175)

$$I_b^2 = \frac{q\Delta f_n\eta_{ff}A_{fp}C_1C_e}{\eta_s\eta_cF_c^2} \int_{\lambda_1}^{\lambda_2} \left[1 - \frac{\varphi_{ms}\lambda}{1.24} \right]^2 \frac{\exp^{-C_2/\lambda T}}{\lambda^5} d\lambda$$

The fixed pattern noise can be written in terms of the background noise as follows:

$$I_f^2 = \left[\frac{MI_b^2}{4q\Delta f_n} \right]^2$$

Where M is the fixed pattern noise modulation factor. Because the modulation factor is defined as the ratio of the rms fixed pattern noise to the rms shot noise due to the background, it represents a measure of the degree of nonuniformity (39:176). The dark or leakage current for a Schottky Barrier device is due almost entirely to thermionic emission and its current density is given by (39:177)

$$J_D = A_R T_{fp}^2 \exp \frac{-q\varphi_{ms}}{kT_{fp}}$$

where A_R is the Richardson emission constant for silicon, T_{fp} is the focal plane temperature, and k is Boltzmann's constant. The current density represented by J_D is very sensitive to temperature and it is this noise source which makes cryogenic ($77K^\circ$) temperatures necessary for optimum performance. The dark current noise is

given by

$$I_D^2 = 2q\eta_{ff} A_{fp} J_D \Delta f_n$$

For large area images, the large image video SNR is defined as (39:177)

$$\text{SNR}_{vo} = \frac{\Delta i}{[I_b^2 + I_F^2 + I_D^2]^{1/2}}$$

which can be written

$$\text{SNR}_{vo} = \frac{K_s \Delta T}{[I_b^2 + I_F^2 + I_D^2]^{1/2}}$$

Now, by definition, $\text{NE}\Delta T$ is defined as the temperature difference for a large target which yields a SNR equal to unity. Setting SNR_{vo} equal to one and solving for ΔT yields

$$\text{NE}\Delta T = \frac{[I_b^2 + I_F^2 + I_D^2]^{1/2}}{K_s}$$

The above derivation is intended to show how the fixed pattern noise is added in quadrature with the other noise sources. Also, the background noise dependence of the fixed pattern noise is made evident. In general, the fixed pattern noise is the dominant noise source (39:169). Any number of additional noise sources may be added in quadrature with the three noise sources described above. These would include kTC noise, a type of thermal noise associated with the charging and discharging of capacitors, readout and transfer noise, and an additive noise often termed the noise floor (39:173).

3.5 Kennedy Model

The Kennedy model is unique in that it combines aspects of both the matched filtering concepts employed in the NVL model and the synchronous integrator approach employed by Rosell and Wilson (40:122). In the form presented below, the Spatial Integration Factor (SIF) and Temporal Integration Factor (TIF) are explicitly represented. Since the Kennedy $\text{NE}\Delta T$ expression doesn't account for response

nonuniformity, its derivation will not be presented.

3.5.1 *Kennedy MRTD* The Kennedy MRTD expression is given as follows

$$\text{MRTD}(f_x) = \frac{\pi \text{SNR}_{th} \text{NE} \Delta T}{4 \text{MTF}(f_x) \text{TIF} \text{SIF}(f_x) \text{SAT}(f_x)} \quad (3.7)$$

where the temporal integration factor TIF is defined as

$$\text{TIF} = (F_R t_E)^{1/2}$$

The spatial integration factor is given by

$$\text{SIF} = \left[\frac{\Omega_{te}}{\Omega_{pe}} \right]^{1/2}$$

where Ω_{te} is the solid angle subtended by the target at the eye and Ω_{pe} is the solid angle of a noise pixel subtended at the eye. For staring arrays, the size of the noise pixel is determined by the detector spacing. The spatial integration factor SIF in the MRTD expression is shown as a function of spatial frequency because Ω_{te} is a function of spatial frequency. For a single bar, Ω_{te} can be given by

$$\Omega_{te}(f) = \frac{7}{4f^2}$$

The saturation term $\text{SAT}(f_x)$ is necessary because the eye/brain cannot perform the spatial integration function when the target area subtends a solid angle at the eye exceeding Ω_{sat} (40:130). This term is essentially unity for high spatial frequencies but reduces the SIF at low spatial frequencies to conform with the results of psychophysical studies (40:122). The functional form of the saturation term is presented below

$$\text{SAT} = \left[\frac{\Omega_{sat}}{\Omega_{sat} + \Omega_{te}} \right]^{1/2}$$

where Ω_{nat} is equal to 225 microsteradians (40:130). A different SIF is required for aperiodic targets at high spatial frequencies, when the target dimensions approach the size of a noise pixel but this is not a problem for standard bar targets (7:1 aspect ratio).

3.5.2 Kennedy Aliasing Treatment In most communications applications, the preferred way to handle aliasing is not to allow it to occur. Images obtained with staring arrays are apt to be afflicted to some extent with spurious response and moiré. The central question is, given that aliasing will occur, how does this effect the spatial frequency dependent sensitivity or MRTD of the system? Before trying to answer that question, some additional background is in order.

3.5.2.1 Post Filtering versus Aliasing One way to eliminate aliasing is to post filter the scene spectra prior to sampling so that the Nyquist criteria is satisfied. This could be accomplished by slightly defocusing the objective lens. It has been shown however that the prefiltering required to eliminate aliasing often does more harm than good (51:252). Kennedy assumes that the impact on recognition is the same whether aliasing is permitted or filtered out prior to display (40:135).

3.5.2.2 Effect of Signal Aliasing Kennedy takes this idea a step further and attempts to determine the loss of recognition that results from undersampling. He claims that the image degradation due to aliasing can be modeled as a coherent noise source for periodic targets and as a random noise source for aperiodic targets. Because noise is introduced into the individual detector elements after sampling, noise aliasing or foldback is not a factor (40:138).

3.5.2.3 Four-Bar Target In an effort to model the laboratory MRTD measurement, we need to quantify the effect that aliasing has on resolving the standard four bar MRTD chart. Does this chart constitute a periodic or aperiodic pattern. Strictly speaking, because of the chart's finite extent, it is an aperiodic pattern.

However, most models assume the four-bar pattern can be replaced by an infinite bar pattern whose transform, by way of Fourier techniques, is easily obtained. The Fourier Transform of both the infinite bar pattern and the four bar pattern are presented in Figure 3.3.

3.5.2.4 Impact on MRTD The Kennedy approach is to treat the four-bar pattern as a periodic scene. In calculating the amount of spurious signal caused by aliasing, he advises the periodic bar "Fourier transform may be replaced for all frequencies expected to show strong aliasing, by $4/\pi$ times a delta function at the fundamental frequency of the aliased four-bar target... (40:137)." This assumption, Kennedy admits, is not very realistic, yet it contains the essence of the problem. Another approach is to treat the four-bar pattern as an aperiodic pattern and computing the noise introduced by aliasing. Following the approach suggested by Borg (8), the $NE\Delta T$ expression is redefined as follows:

$$NE\Delta T = [NE\Delta T_s^2 + NE\Delta T_a^2]^{1/2}$$

where $NE\Delta T_s$ is the system noise figure calculated without aliasing as before and $NE\Delta T_a$ represents the noise introduced by signal aliasing. The $NE\Delta T$ due to aliasing may be given by

$$NE\Delta T_a = \Delta T \int_{f_{nvq}}^{\infty} MTF(f)BAR(f)df$$

where ΔT is the temperature difference between the background and target, and $BAR(f)$ is the Normalized Fourier transform of the four-bar pattern. Since the amount of aliased signal, for a given frequency, is proportional to the target radiance which influences MRTD, an iterative procedure is necessary to calculate $MRTD_a$ from MRTD. There is some question, however, concerning how damaging aliasing is in terms of loss of recognition. The problem with treating the problem in the frequency domain is that "... the viewer is influenced primarily by the spatial content of the reproduction rather than the frequency content. Although a moiré pattern

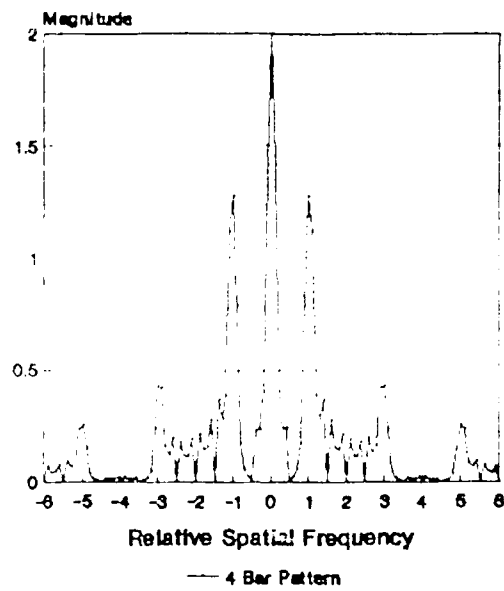
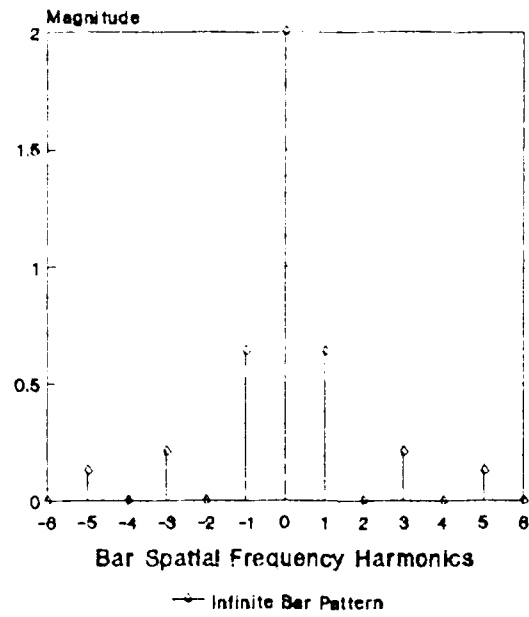


Figure 3.3. Transforms of Infinite and 4-Bar Patterns

might occupy the same frequency domain as the true signal, it does not occupy the same space in the image plane, as is the case with additive noise.”(51:252) Further validation of the Kennedy-Borg approach is needed before it is incorporated into other models. As will be seen in the model comparison, incorporating aliasing effects might be considered overkill since the models tend to overpredict the MRTD near the nyquist frequency.

3.6 Summary

This chapter introduced essential elements of the MRTD modeling process, discussed eye/brain SNR enhancement mechanisms, MTF and sensitivity relations. Three staring array models were presented in greater detail. The NE Δ T derivation for the Rosell model was presented to highlight the nonuniformity treatment, which well represents the manner in which nonuniformity is treated in other models. Also, the Kennedy aliasing treatment is presented and some minor modifications are introduced. The next chapter attempts to evaluate the three models by comparing the MRTD predictions against those obtained by direct measurement.

IV. Model Comparisons

4.1 Introduction

This chapter discusses the modeling process and emphasizes the importance of validation in this process. Through the use of experimentally measured MRTD curves and the necessary camera parameters, the predictive power of the MWIR, Kennedy, and Rosell models is examined. Significant trends and deviations are noted. All the MRTD measurements presented in this chapter were performed by the Electro-Optical Techniques Group, WRDC/AARI, Wright-Patterson AFB, OH.

4.2 Modeling Process

The first step in modeling is to establish a modeling parameter or criterion. This was accomplished by choosing the sensor system MRTD as the modeling criterion. Through extensive research and the use of existing staring array models, critical parameters which strongly influence MRTD have been identified. The relationships among these parameters are more or less established by the models themselves. How well these models actually predict MRTD is the next area of inquiry. In a sense, this step might be considered model validation though the term *validation* implies the use of a much larger data set than set forth here. Interestingly enough, it is this lack of validation (due in part to hardware (staring array camera) unavailability) that has greatly slowed the progress in modeling staring array cameras. Since modeling is an iterative process, the results from this cycle should provide feedback for succeeding modeling efforts.

4.3 Camera-One Comparison

The first staring array camera, herein referred to as Camera-One, used in the model comparison is a Rome Air Development Center (RADC) 160 x 244 detector element Platinum Silicide camera using a 100mm focal length lens. Camera-Two

Description	Parameter
Number of Vertical Detectors	214
Number of Horizontal Detectors	160
Vertical Detector Size (Active)	25 μm
Vertical Detector Pitch	40 μm
Horizontal Detector Size (Active)	50 μm
Horizontal Detector Pitch	80 μm
Array Fill Factor	39%
Vertical Detector Pitch	5.55° 96.8 mrad
Horizontal Detector Pitch	7.46° 130.2 mrad
Focal Length of Objective Lens	100 mm
F-number	1.8
Instantaneous VFOV	.25 mrad
Instantaneous HFOV	.5 mrad
Vert Detector Angular Pitch	.4 mrad
Horiz Detector Angular Pitch	.8 mrad
Noise Equivalent Temperature	.055° C
Nominal Cutoff (Nyquist) Vertical	1.25 cycles/mrad
Nominal Cutoff (Nyquist) Horizontal	.625 cycles/mrad

Table 4.1. Camera-One Parameter Listing

is essentially the same camera with a 299mm focal length lens. Table 4.1 contains a detailed listing of the essential camera parameters used in the model comparison. Since the measured NE Δ T values were available for these cameras, predicted sensitivity results were not necessary. Predicted values of NE Δ T were calculated for Camera-One within 20% but estimates were made regarding certain noise parameters (dark current, degree of nonuniformity, and the like). Table 4.2 lists the measured vertical and horizontal MRTD values for Camera-One. Note the increased vertical resolution yields improved MRTD only for higher spatial frequencies. At low spatial frequencies, the influence of sensitivity dominates whereas at higher spatial frequencies, the fall-off in frequency response becomes more influential.

Figure 4.1 shows the predicted versus measured vertical MRTD for Camera-One. None of the models appears to be a clear winner in this one though both

Test Spatial Frequency cycles/mrad	Vertical MRTD °C	Horizontal MRTD °C
0.25	0.02	0.02
0.50	0.04	0.07
0.75	0.05	—
1.0	0.06	—

Table 4.2. Camera-One Measured Values (52:7)

the Rosell and MWIR model appear close at .75 cycles/mrad. These two models also seem to have the same difficulties as the NVL model at low spatial frequencies. The Kennedy model is pessimistic throughout the range. All the models predict pessimistically (high) for the highest spatial frequency MRTD. Figure 4.2 compares the measured horizontal MRTD against the predicted results obtained using the MWIR, Kennedy and Rosell models. Here it looks like the measured values are well bracketed, again with the Kennedy model yielding the higher MRTD values. With only two measured points, it is difficult to establish any trend. As before, the MWIR and Rosell model are optimistic (low) at the lower spatial frequencies.

4.4 Camera-Two Comparison

The second staring array camera, herein referred to as Camera-Two, is a Rome Air Development Center (RADC) 160 x 244 Platinum Silicide camera with a 299mm focal length lens. Because of different transmission characteristics of the 299mm lens, the NEΔT for this camera is slightly larger. The higher resolution of this camera yields more data points for comparison purposes. Table 4.3 contains a detailed listing of the essential parameters for Camera-Two. Table 4.4 lists the measured vertical and horizontal MRTD values for Camera-Two. Again, note the similarity in measures at low spatial frequencies where sensitivity dominates. At higher spatial frequencies, the benefits of small detector size and pitch become pronounced. The last MRTD measure in the vertical direction is surprising and will no doubt be missed by the models. Figure 4.3 shows the predicted versus measured vertical MRTD for

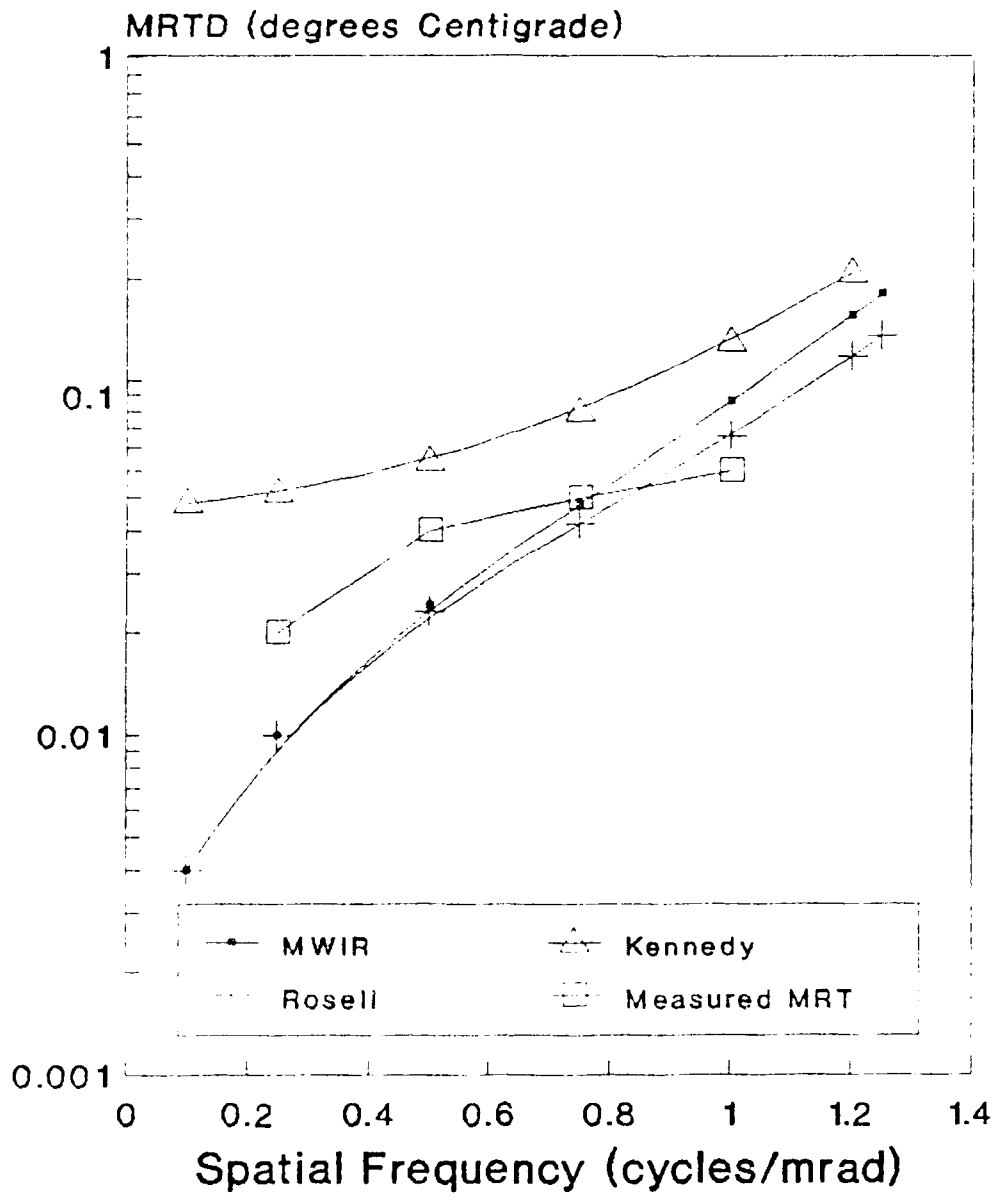


Figure 4.1. Camera-One Vertical MRTD Comparison

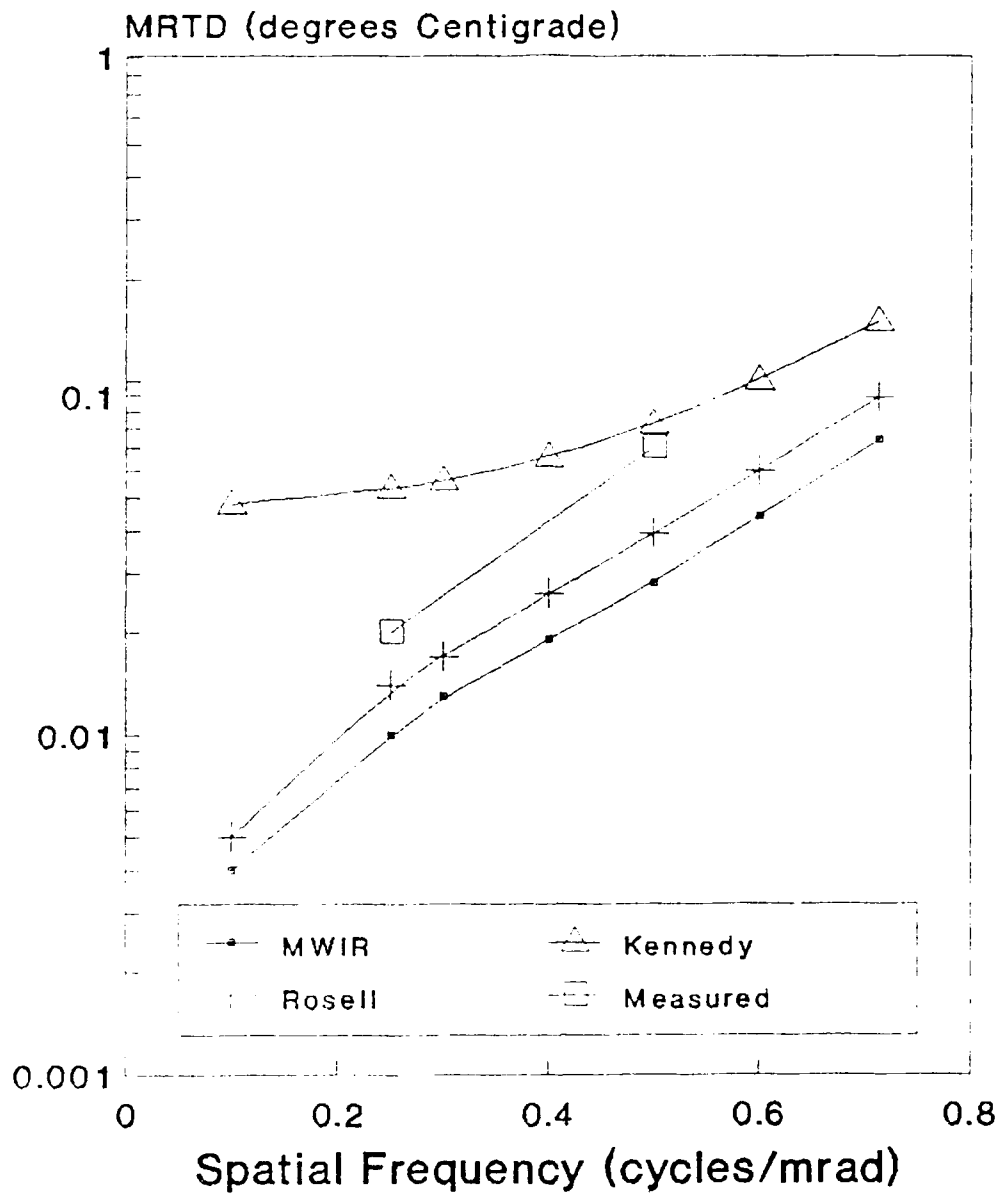


Figure 4.2. Camera-One Horizontal MRTD Comparison

Description	Parameter
Number of Vertical Detectors	244
Number of Horizontal Detectors	160
Vertical Detector Size (Active)	25 μm
Vertical Detector Pitch	40 μm
Horizontal Detector Size (Active)	50 μm
Horizontal Detector Pitch	80 μm
Array Fill Factor	39%
Vertical Field of View (VFOV)	1.91° 33.3 mrad
Horizontal Field of View (HFOV)	2.56° 44.7 mrad
Focal Length of Objective Lens	299 mm
F-number	2.35
Instantaneous VFOV	.0836 mrad
Instantaneous HFOV	.167 mrad
Vertical Detector Angular Pitch	.134 mrad
Horizontal Detector Angular Pitch	.268 mrad
Noise Equivalent Temperature	.08° C
Nominal Cutoff (Nyquist) Vertical	3.73 cycles/mrad
Nominal Cutoff (Nyquist) Horizontal	1.86 cycles/mrad

Table 4.3. Camera-Two Parameter Listing

Test Spatial Frequency cycles/mrad	Vertical MRTD °C	Horizontal MRTD °C
0.25	0.02	0.02
0.50	0.03	0.03
0.75	0.03	0.04
1.0	0.04	0.05
1.5	0.04	0.07
2.0	0.08	0.18
2.5	0.09	—
3.0	0.15	—
3.5	0.20	—
4.0	0.20	—

Table 4.4. Camera-Two Measured Values (52:7)

Camera-Two. Here, at least for the higher spatial frequencies, the models do a better job. Again, the MWIR and Rosell model predict low at low spatial frequencies. The Kennedy model seems to give the best match overall with only the first and last data points deviating significantly from the measured values. As with the Camera-One measurements, at the highest spatial frequency, all the models predict high. Figure 4.4 shows the predicted versus measured horizontal MRTD for Camera-Two. Again, the Rosell and MWIR model predict a MRTD much lower than measured at the lower spatial frequencies. The Kennedy model, which was undistinguished in the Camera-One comparisons, seems to predict the Camera-Two MRTD fairly well, or at least, better than the other models. Here, however, the measured MRTD for the highest spatial frequency surpasses the predicted values. Since resolution dominates in the high spatial frequency region, this might be the result of an error in the modeled MTF.

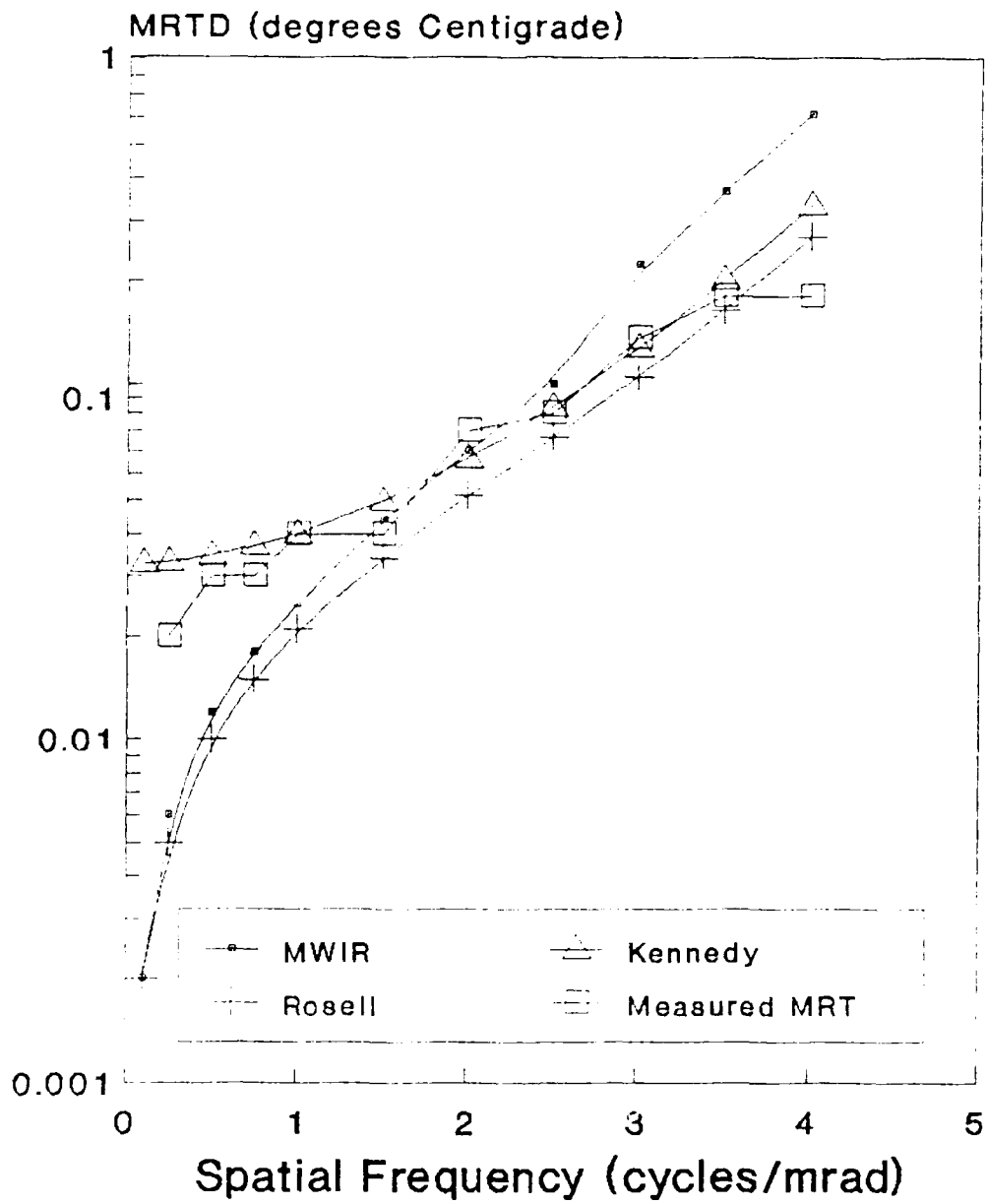


Figure 4.3. Camera-Two Vertical MRTD Comparison

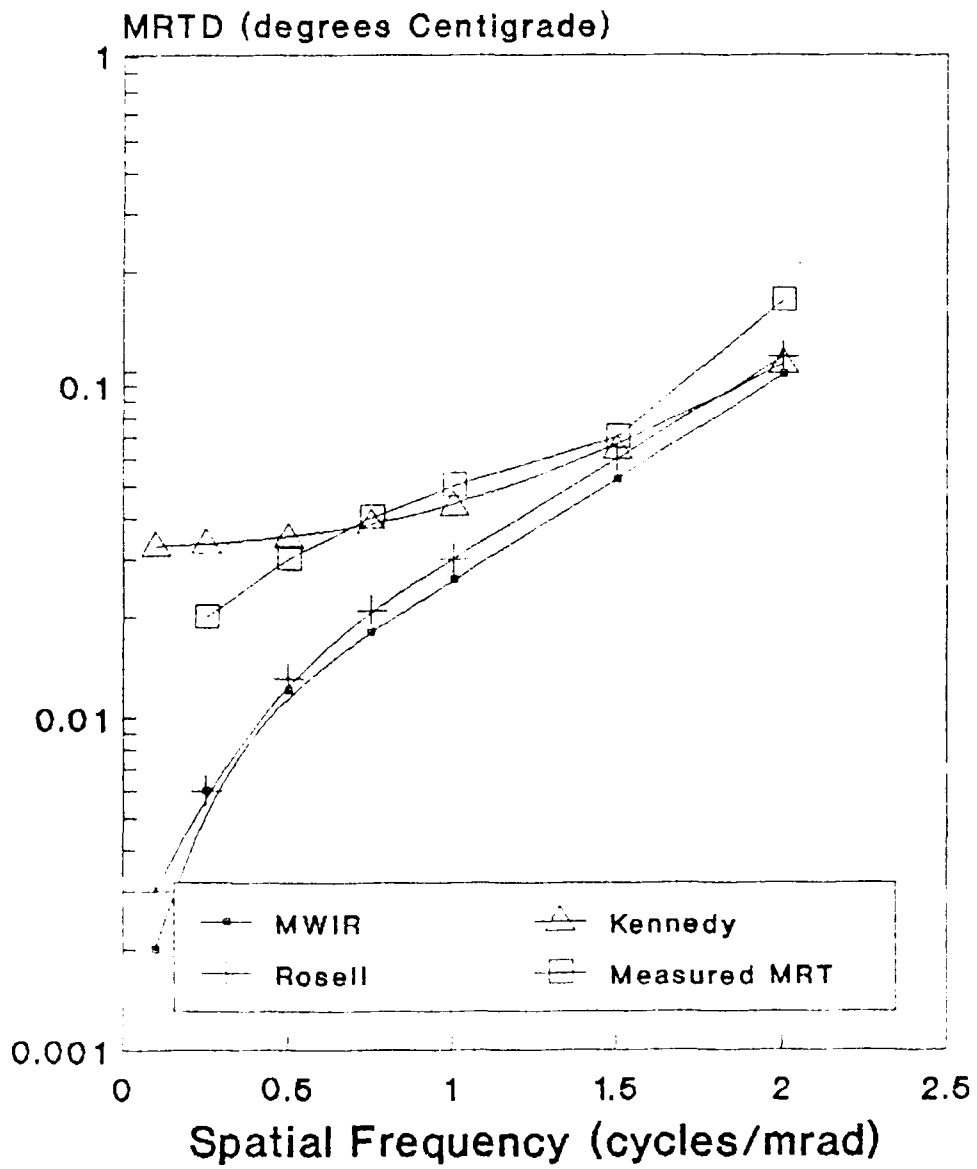


Figure 4.4. Camera-Two Horizontal MRTD Comparison

Description	Parameter
Number of Vertical Detectors	256
Number of Horizontal Detectors	256
Vertical Detector Size (Active)	29.24 μm
Vertical Detector Pitch	30.0 μm
Horizontal Detector Size (Active)	29.24 μm
Horizontal Detector Pitch	30.0 μm
Array Fill Factor	95%
Vertical Detector Angular Pitch	1.43° 25.0 mrad
Horizontal Detector Angular Pitch	1.46° 25.5 mrad
Focal Length of Objective Lens	299 mm
F-number	2.1
Instantaneous VFOV	.0978 mrad
Instantaneous HFOV	.0978 mrad
Vertical Detector Angular Pitch	.1 mrad
Horizontal Detector Angular Pitch	.1 mrad
Noise Equivalent Temperature	.08° C
Nominal Cutoff (Nyquist) Vertical	5 cycles/mrad
Nominal Cutoff (Nyquist) Horizontal	5 cycles/mrad

Table 4.5. Camera-Three Parameter Listing

4.5 Camera-Three Comparison

The results of the first two comparison exercises are perhaps inconclusive. Adding to the confusion is the matter of MTF uncertainty. In order to remove differences in MRTD predictions that might result from the variance between predicted and measured MTF, the Camera-Three Comparisons will use laboratory measured MTF values. With this approach, it is hoped the MRTD models can be evaluated directly to see which model translates the $NE\Delta T$ and MTF measures into the most accurate MRTD. The third staring array camera, herein referred to as Camera-Three, is a Rome Air Development Center (RADC) 256 x 256 Platinum Silicide camera with a 299mm focal length lens. Table 4.5 contains a detailed listing of the essential parameters for Camera-Three. Unlike the previous two cameras, which had monolithic arrays, Camera-Three has a hybrid array. Although this allows for higher fill factors,

Test Spatial Frequency cycles/mrad	Vertical MRTD °C	Horizontal MRTD °C
0.25	0.033	0.028
0.50	0.052	0.019
0.75	0.080	0.024
1.0	0.099	0.052
1.5	0.113	0.062
2.0	0.137	0.071
2.5	0.104	0.094
3.0	0.127	0.113
3.5	0.179	0.127
4.0	0.400	0.151
4.5	0.400	0.16
5.0	0.494	0.155

Table 4.6. Camera-Three Measured Values (53:14)

the amount of transfer noise and the degree of nonuniformity are generally higher. Table 4.6 lists the measured vertical and horizontal MRTD values for Camera-Three. Note that the MRTD values in the vertical direction are quite a bit higher than the horizontal. This is contrary to what one would expect based on the measured MTFs which implied better vertical response. Although the MTFs would be approximately equal based on detector spacing, the horizontal MTF is reduced further by the electronics MTF (whereas the vertical is not). Further investigation by the Avionics Lab showed that the discrepancy resulted from asymmetrical noise within the array. The measured fixed pattern noise power in the vertical direction was twice that found in the horizontal direction and the vertical temporal noise power four times the horizontal value. Figure 4.5 shows the predicted versus measured vertical MRTD measurements for Camera-One. All the models predict low at the lower spatial frequencies. Since the higher noise power in the vertical direction hasn't been accounted for in the models, agreement with this data doesn't necessarily reflect well on the model. In this case, the MW R model shows the best agreement. Both the Rosell and Kennedy models predict low, as they should, based on the measured

MTF values. Figure 4.6 shows the same information for the horizontal MRTD. Here, with more modest noise figures, the MWIR model overpredicts for most the spatial frequency range. The Kennedy model is consistently optimistic for both directions. The Rosell model is the nearest to the measured values over the frequency range in terms of minimum mean square error. Contini and Hoznik (33:73) recommend combining the vertical and horizontal MRTD in the following manner to arrive at a single measure of system performance:

$$\text{MRT}_c = \left[\frac{2}{\text{MRT}_h^{-2} + \text{MRT}_v^{-2}} \right]^{1/2}$$

When the predicted and measured results are combined in this manner, and the mean square error calculated, the Rosell model yields the closest fit to the measured data.

4.6 Summary

Two things regarding the model comparison are particularly noteworthy. First, from just viewing the graphical results, no one model stands out as the being that much better than any of the others. The second point worth mentioning is, for whatever reason, the agreement wasn't much better when the measured MTFs were used. In any contest, there has to be a winner, so I've devised a way in which the relative model performance might be measured which is consistent with mean squared error comparisons. For each of the six sets of data (3 sets of vertical and horizontal measurements), a cumulative error calculation was made to rank order the model performance; a '1' indicates lowest cumulative error for those measures and a '3' indicates highest cumulative error. The results are contained in Figure 4.7. The average scores for the models in this comparison are 1.5 for the Rosell Model, 2 for the Kennedy Model, and 2.5 for the MWIR model. Granted, the data set is much too small to make any sweeping judgments about any of the models, but the Rosell model did well to avoid any of the lowest scores.

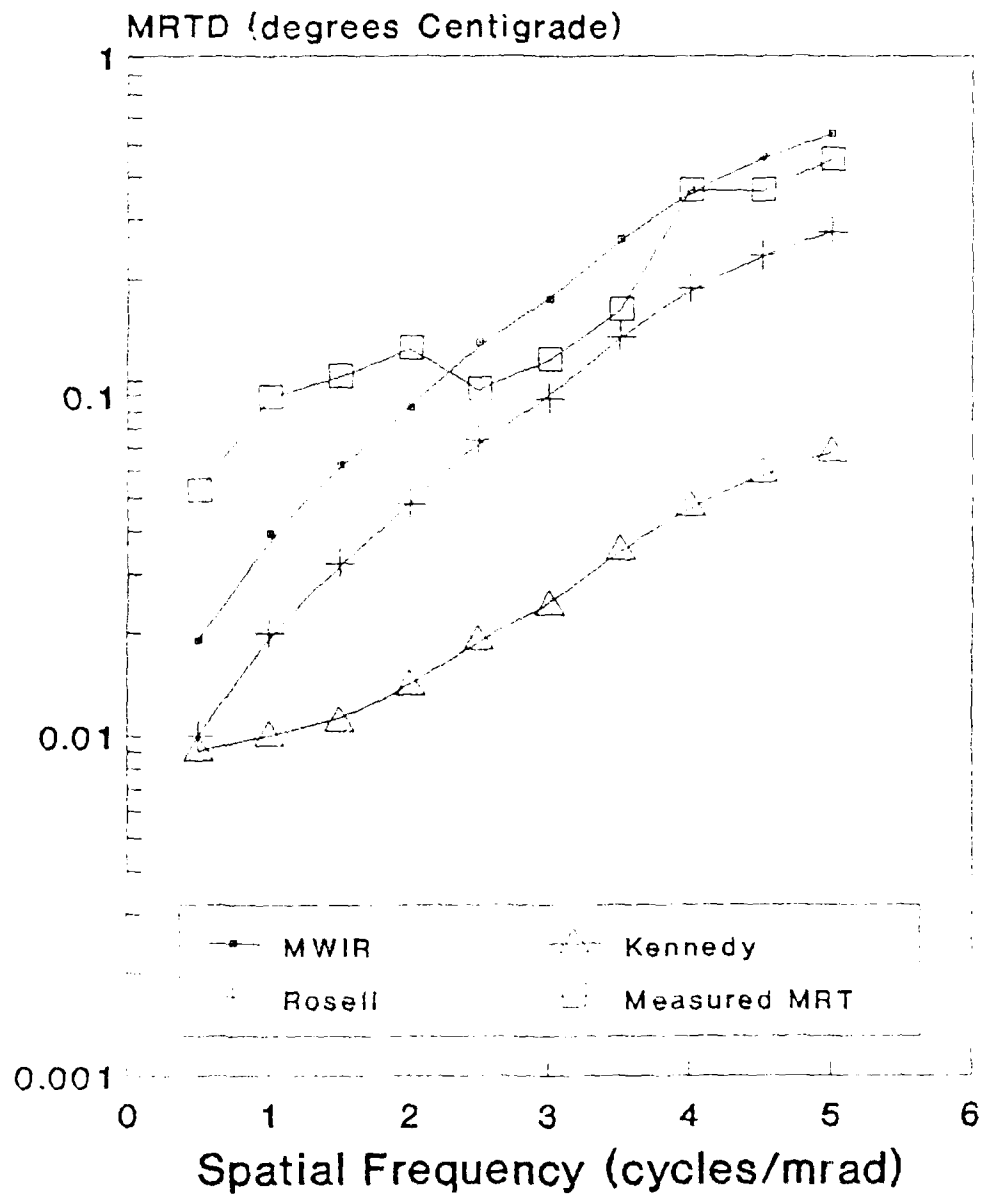


Figure 4.5. Camera-Three Vertical MRTD Comparison

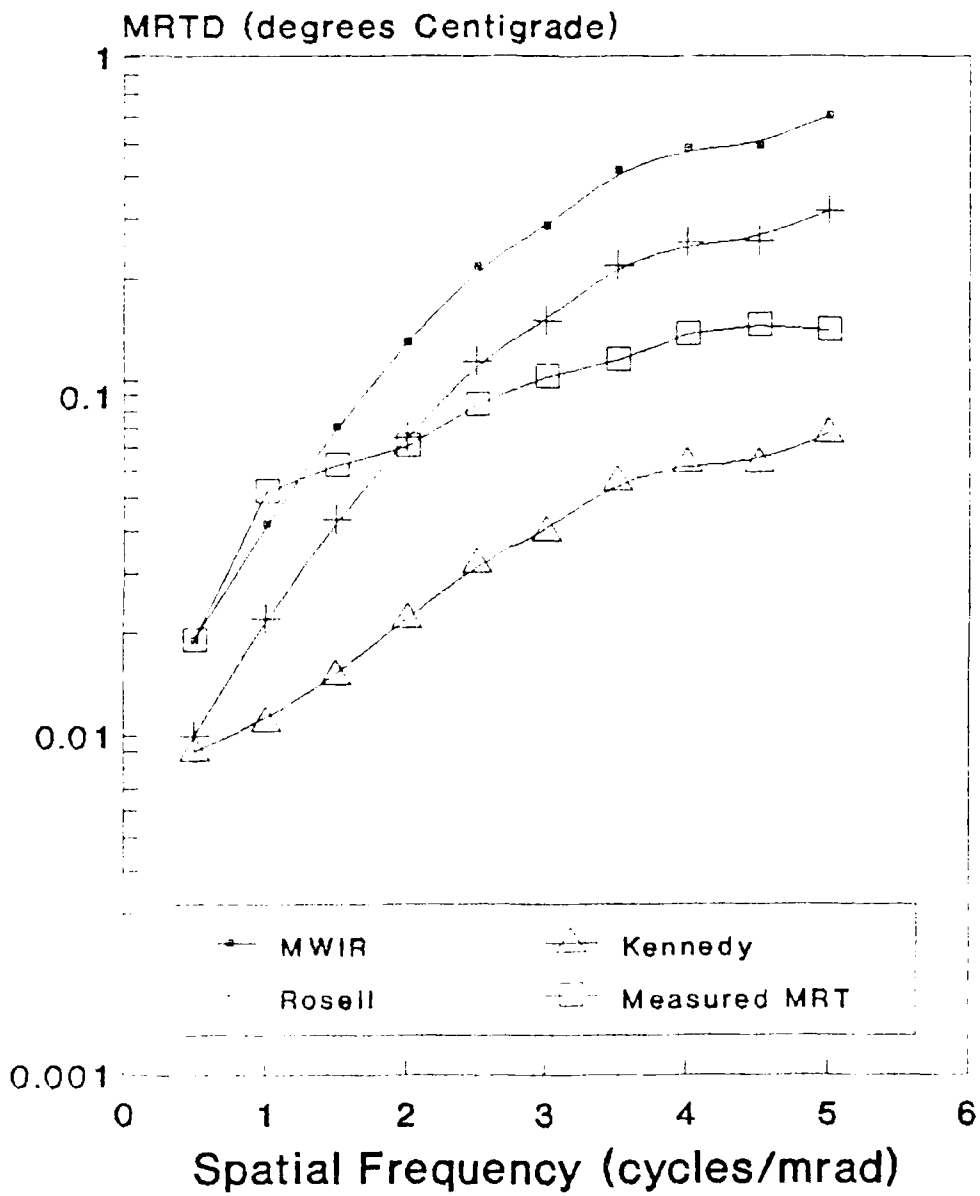


Figure 4.6. Camera-Three Horizontal MRTD Comparison

Model	Cam1V	Cam1H	Cam2V	Cam2H	Cam3V	Cam3H
MWIR	3	2	3	3	1	3
Kennedy	2	3	1	1	3	2
Rosell	1	1	2	2	2	1

Table 4.7. Model Performance

V. *Conclusions and Recommendations*

5.1 *Conclusions*

This thesis has shown that we are still a long way from properly characterizing staring focal plane array performance. The variance between the measured and predicted results was in general high, particularly at the extreme ranges in spatial frequency. The difference in shape between the measured and predicted results would seem to imply the existence of fundamental flaws in the staring array modeling expressions in general and the operator interface submodels in particular. Perhaps most indicting are the results of the Camera-Three comparisons. Even when the measured square-wave response was used instead of the theoretical MTF expressions, the variance between measured and predicted results was still high. The best Camera-3 match, the Kennedy horizontal MRTD prediction, was an average of 20% off over the ten MRTD data points. The Rosell model was off an average of 45% in the horizontal direction and the MWIR a whopping 157%. The results in the vertical direction were in general much worse. However, in fairness to all three models, the increased noise power in the vertical direction in Camera-Three wasn't accounted for in the model. This is significant because, even with this knowledge, there is no validated way to include asymmetrical noise distributions into the MRTD expression. It is clear that, in addition to work on the MRTD expressions themselves, a more realistic description of the noise is required. This supports the contention by Boreman (29) that reducing the fixed pattern noise contribution to a simple rms value throws away too much information. A two-dimensional noise figure is required to better describe the performance of arrays with asymmetrical noise distributions such as that found in Camera-3. Of all the models examined, the Rosell model would have to be termed the better overall. However, the Rosell model, much like the MWIR and other NVL derivatives, is generally optimistic (low) at low spatial frequencies. An improved eye MTF along with a limitation to the spatial integration

at low spatial frequencies would help improve the model's predictive power. This, however, doesn't solve the problems evident at higher spatial frequencies. Because of the models' tendency to overpredict the MRTD near the nyquist frequency, there didn't seem to be much sense in adding an aliasing factor. Part of the reason for the lower MRTD measurements at or near f_{nyq} might result from the manner in which the measures are made. Earlier, it was mentioned that the phase between the target and sampling lattice was critical at or near f_{nyq} . By adjusting the phase for maximum response, the aliased components actually reinforce the signal and improve the bar visibility. This would explain how the measured MRTD could be .2 at both 3.5 and 4 cycles/mrad during the vertical Camera-Two measurements. Even if the models didn't overpredict at high spatial frequencies, further data is required to validate the aliasing approach introduced by Kennedy and modified by Borg.

5.2 Recommendations

The following items are the major modeling problem areas and, through this research, the nature of the modeling problem can now be more precisely stated and suggestions can be made regarding the direction of future modeling research.

- Operator Interface
- FPA Noise Characterization

The operator interface is still not well understood but there is reason for some optimism. With the Rosell model results and the findings presented by Vortman and Bar-Lev (10) regarding the *Limited Synchronous Integrator Model*, there is reason to believe that an improved operator interface can be achieved by either adapting the Vortman Limited Synchronous Integrator Model for staring arrays or modifying the Rosell model by limiting spatial integration at low spatial frequencies. All the models would benefit from an improved eye MTF for use in system MTF expression and the noise filtering functions. Just how (MTF or empirical correction factors) to

account for the nonlinearities (edge enhancement, adaptive spatial filtering) introduced by the eye/brain is not clear. How far can linear systems theory and the MTF concept be extended in describing the eye/brain behavior? How much variability is there in terms of individual eye/brain response? These are questions that have not been answered. A major study by Horst on the MTF of the eye is scheduled to be published in SPIE soon. The study, associated with the LANTIRN program, supposedly involved thousands of test subjects.

As far as FPA noise characterization is concerned, work remains on characterization of noise in two directions, both spatial and temporal. Also, regarding the aliasing effects upon imagery, there is still some doubt that frequency domain reasoning can answer the question of how aliasing in the frequency domain affects images in the spatial domain. More empirical data on the relationship between aliasing and pattern recognition is required. Also deserving a closer look is the phase dependence of sampling and the common practice of peaking the signal by adjusting the sampling phase. Would MRTD models do better at higher spatial frequencies if, as a condition of the measurement, the phase is chosen midway between the maximum and minimum response? Also, since there is a certain amount of inherent variability in the MRTD measures made between different operators (and the same operators on different days), the question arises as to how close can one model something as variable as MRTD? How close is close enough? More research is necessary to answer these questions. Perhaps this highlights the danger of using MRTD, a subjective measure, as the summary measure for TIS systems. More research is also required to identify objective correlates with staring array performance.

Bibliography

1. Shukaker, David L. and James T. Wood. "Overview of Current IR Analysis Capabilities and Problem Areas," *Proceedings of SPIE*, 890: 74-80 (1988).
2. NATO-AC/243 (Panel 4)D/217 Joint Task 2, "Advanced Thermal Imager Performance Modeling Study," Report ADB123651 (May 1988).
3. Biberman, Lucien M. and Sol Nudelman. *Photoelectronic Imaging Devices*. New York: Plenum Press, 1974.
4. Lloyd, Michael J. *Thermal Imaging Systems*. New York: Plenum Press, 1975.
5. Biberman, Lucien M. , ed. *Perception of Displayed Information*. New York: Plenum Press, 1973.
6. Cuthbertson, Glenn M. , Leslie G. Shadrake, and Neil J. Short. "A technique for the objective measurement of MRTD," *Proceedings of SPIE*, 590: 179-188 (1985).
7. Newbery, A. R. , and R. McMahon. "Use of minimum resolvable temperature difference (MRTD) for the evaluation and specification of thermal imaging systems," *Proceedings of SPIE*, 274: 268-272 (1981).
8. Borg, Eric J. , Joel S. Davis, and Bryan D. Thompson. "Modeling approaches to thermal imaging systems," *Proceedings of SPIE*, 636: 2-16 (1986).
9. Hepfer, Kenneth C. "A New TIS Technical Performance Model," Paper Presented at the IRIS Specialty Group on Infrared Imaging, 2-3 December 1981.
10. Vortman, J. G. and A. Bar-Lev. "Improved minimum resolvable temperature difference model for infrared imaging systems," *Optical Engineering*, 26: 492-498 (June 1987).
11. McCracken, William and Leo Wajsfelner. "MRTD as a figure of merit," *Proceedings of SPIE*, 636: 31-35 (1986).
12. Humphreys, R. G. , "Specification of Infrared Detectors and Arrays," *Infrared Physics*, 28: 29-35 (1988).
13. Kruer, M. R. , D. A. Scribner and J. M. Killiany. "Infrared focal plane array technology development for Navy Applications," *Optical Engineering*, 26: 81-91 (March 1987).
14. Gaskill, Jack D. *Linear Systems, Fourier Transforms, and Optics*. New York: John Wiley & Sons, 1978.
15. Goodman, Joseph W. *Introduction to Fourier Optics*. New York: McGraw-Hill, 1968.

16. Williams, T. L. "Assessing the Performance of Complete Thermal Imaging Systems" *Proceedings of SPIE*, 590: 172-175 (1985).
17. Montgomery, Duane W. "Sampling in imaging systems," *Journal of the Optical Society of America*, 65: 700-706 (Jun 1975).
18. Wittenstein, W. *et al.* "The definition of the OTF and the measurements of aliasing for sampled imaging systems," *Optica Acta*, 29: 41-50 (1982).
19. Bradley, D. J. , C. J. Braddley, and P. Dennis. "The Modulation Transfer Function of Focal Plane Array Systems," *Proceedings of IEEE*, 807: 33-41 (1987).
20. Cox, J. Allen. "Advantages of hexagonal detectors and variable focus for point source location," *Proceedings of SPIE*, 750: 62-72 (1987).
21. Mersereau, Russel M. "Hexagonal pixels, arrays, and sampling," *Proceedings of SPIE*, 750: 57-61 (1987).
22. Marshall, Donald E. "Focal plane array design for optimum system performance," *Proceedings of SPIE*, 226: 66-73 (1980).
23. Seib, David H. "Charge Diffusion Degradation of Modulation Transfer Function in Charge Coupled Imagers," *IEEE Transactions on Electron Devices*, 21: 210-216 (Mar 1974).
24. Thurlow, Paul E. "Principles and applications of carrier diffusion modeling," *Proceedings of SPIE*, 892: 2-6 (1988).
25. Barbe, David F. "Imaging Devices Using the Charge Coupled Concept," *Proceedings of IEEE*, 63: 38-67 (1975).
26. Mooney, Jonathan M. and Eustace Deraniak. "Comparison of the performance limit of Schottky-barrier and standard infrared focal plane arrays," *Optical Engineering*, 26: 223-227 (Mar 1987).
27. Milton, A. F. , F. R. Barone and M. R. Kruer. "Influence of non-uniformity on infrared focal plane array performance," *Optical Engineering*, 24: 855-858 (1985).
28. Murguia, James E. and William S. Ewing. "Statistical characterization of a large PtSi focal plane array," *Proceedings of SPIE*, 782: 121-128 (1987).
29. Boreman, Glenn D. "Fourier spectrum techniques for characterization of spatial noise in imaging arrays," *Optical Engineering*, 26: 985-991 (Oct 1987).
30. Mooney, J. M. , F. D. Shepherd, W. S. Ewing, J. E. Murguia, and J. Silverman. "Responsivity Nonuniformity Limited Performance of Infrared Staring Cameras," *To Be Published in Optical Engineering*.
31. Cross, E. F. , and T. M. Reese. "Figures of merit to characterize integrating image sensors: a ten-year update," *Proceedings of SPIE*, 972: 195-206 (1988).

32. Deraniak, Eustace L. and Devon G. Crowe. *Optical Radiation Detectors*. New York: Wiley & Sons, 1984.
33. Contini, Casey and Richard Honzik. "Staring FPA Modeling Capability," *Proceedings of SPIE*, 636: 60-70 (1986).
34. Thevdt, Tom A. , Charles T. Willoughby, Michael M. Salcido, and Eustace L. Deraniak. "Computer model of focal plane array," *Proceedings of SPIE*, 819: 250-261 (1987).
35. NATO Document AC/243(Panel 4)D/218 "Report on the State of the Art of the Assessment of Staring Arrays and Sampled Infrared Imaging Systems: an RSG.16 Overview," Report ADB123808 (Jun 1988).
36. Hoover, C. , J. Ratches, F. Shields, K. Mayo. "Night Vision and Electro-Optics Laboratory (NVEOL) performance model and its use," *Proceedings of SPIE*, 327: 2-8 (1982).
37. Lucius, C. E. and E. W. Kopala. "Middle Wave Infrared Sensor Performance Model Usage Manual," EO Sensor/ATR Science Development Program, F33615-86-C-1051.
38. Cantella, Michael J. "Infrared focal plane array system performance modeling." *Proceedings of SPIE*, 327: 40-58 (1982).
39. Rosell, Frederick A. "Psychophysical Periodic Model for Platinum Silicide Staring Arrays," *Proceedings of IRIS Imaging*. 169-186 (1987).
40. Kennedy, Howard V. "Two-Dimensional Modeling of FLIR Systems," *Proceedings of IRIS Imaging*. 113-142 (1983).
41. Flaherty, Richard T. and Walter R. Lawson. "Recognition performance of a staring forward looking infrared system (FLIR)," *Proceedings of SPIE*, 267: 99-106 (1981).
42. Lucius, C. E. and E. W. Kopala. "Middle Wave Infrared Sensor Performance Model Analyst Manual," EO Sensor/ATR Science Development Program, F33615-86-C-1051.
43. Ratches, J. A. *et al.* , "Night Vision Laboratory Static Performance Model for Thermal Viewing Systems," Report ADA011212 (April 1975).
44. Orlando, H. J. and J. M. Voss. "Modulation Transfer Function Model for Staring Focal Plane Arrays," *Proceedings of IRIS Detector*, 2: 267-278 (1984).
45. Ho, John Y., Lawson, Walter and Frank Shields. "Sampling Effects on Bar Charts and Scenes," *Proceedings of IRIS Imaging*. 95-111 (1983).
46. Shaham, Y. J. and L. M. Woody. "MRT for Second Generation Systems," *Proceedings of IRIS Imaging*. 155-164 (1981).
47. Vortman, J. and A. Bar-Lev. "Optimal electronics response for parallel thermal imaging systems," *Optical Engineering*, 23: 431-435 (Jul/Aug 1984).

48. Rosell, F. and G. Harvey. "The fundamentals of thermal imaging systems," Appendix D, Naval Research Laboratory Report ADA073763, (1979).
49. Kornfeld, G. H. and W. R. Lawson. "Visual-Perception Models," *Journal of the Optical Society of America*, 61: 811-820 (June 1971).
50. NATO Document AC/243(Panel IV/RSG.7)D/17 "A Comparison of Models Predicting Thermal Imager Performance (COMOD of RSG.7)," Report ADB067240 (July 1981).
51. Barbe, D. F. and S. B. Campana. "Imaging Arrays Using the Charge Coupled Concept," in *Advances in Image Pickup and Display*, B. Kazan, ed. , pp. 171-296, Academic Press, New York (1977).
52. Yasuda, Brian. *Laboratory Characterization of Two RADC 160 x 244 Platinum Silicide Sensors*," Report No. AFWAL-TR-88-1033, pp. 1-57, April 1987.
53. Yasuda, Brian. *Laboratory Characterization of RADC PtSi Sensor with Hughes 256 x 256 Array*," Report No. WRDC-TM-89-1033, pp. 1-74, June 1989.

Vita

Capt John Murphy [REDACTED] He was graduated from Notre Dame University with a Bachelor's degree in Electrical Engineering. He entered the Air Force in 1984 and was assigned to the Air Force Technical Applications Center (AFTAC) at Patrick AFB. While there he managed the communication subsystem for the Global Subsurface System (GSS), an underground nuclear test monitoring system. He received his Master's in Engineering Management from the Florida Institute of Technology in May 1987 and entered AFIT in June 1988. He is married to Laura Blanton of Sikeston Missouri and has two children, Anna and Jack.

[REDACTED]

[REDACTED]

REPORT DOCUMENTATION PAGE

Form Approved
OMB No. 0704-0188

1. REPORT SECURITY CLASSIFICATION Unclassified		1b. RESTRICTIVE MARKINGS	
2a. SECURITY CLASSIFICATION AUTHORITY		3. DISTRIBUTION/AVAILABILITY OF REPORT Approved for public release; distribution unlimited	
2b. DECLASSIFICATION/DOWNGRADING SCHEDULE			
4. PERFORMING ORGANIZATION REPORT NUMBER(S) AFIT/GEO/ENP/89D-3		5. MONITORING ORGANIZATION REPORT NUMBER(S)	
6a. NAME OF PERFORMING ORGANIZATION School of Engineering	6b. OFFICE SYMBOL (if applicable) AFIT/ENP	7a. NAME OF MONITORING ORGANIZATION	
6c. ADDRESS (City, State, and ZIP Code) Air Force Institute of Technology (AU) Wright-Patterson AFB, OH 45433-6583		7b. ADDRESS (City, State, and ZIP Code)	
8a. NAME OF FUNDING/SPONSORING ORGANIZATION WRDC	8b. OFFICE SYMBOL (if applicable) AARI	9. PROCUREMENT INSTRUMENT IDENTIFICATION NUMBER	
8c. ADDRESS (City, State, and ZIP Code) Wright-Patterson AFB, OH 45433		10. SOURCE OF FUNDING NUMBERS	
		PROGRAM ELEMENT NO.	PROJECT NO.
11. TITLE (Include Security Classification) STARING FOCAL PLANE ARRAY SYSTEM MODELING			
PERSONAL AUTHOR(S) John G. Murphy, Capt, USAF			
13a. TYPE OF REPORT	13b. TIME COVERED FROM _____ TO _____	14. DATE OF REPORT (Year, Month, Day) 1989, December	15. PAGE COUNT 70
16. SUPPLEMENTARY NOTATION			
17. COSATI CODES		18. SUBJECT TERMS (Continue on reverse if necessary and identify by block number) Focal Plane Arrays, Infrared Imaging System Modeling, Thermal Imaging System Characterization, Minimum Resolvable Temperature Difference (MRTD) Prediction	
FIELD	GROUP		
09	05		
19. ABSTRACT (Continue on reverse if necessary and identify by block number) This report analyzes the problems of modeling staring focal plane array systems. Two problem areas are highlighted; the difficulty in modeling the operator interface and the inadequate characterization of focal plane array noise sources. The effects of aliasing, response nonuniformity, and the two-dimensional nature of the spatial and temporal noise require more sophisticated handling than found in present models. Three staring array models were used to predict the Minimum Resolvable Temperature Difference (MRTD) for three Platinum Silicide staring array cameras. The predictions were then compared, analyzed, and suggestions for model improvement were made.			
20. DISTRIBUTION/AVAILABILITY OF ABSTRACT <input checked="" type="checkbox"/> UNCLASSIFIED/UNLIMITED <input type="checkbox"/> SAME AS RPT <input type="checkbox"/> DTIC USERS		21. ABSTRACT SECURITY CLASSIFICATION Unclassified	
22a. NAME OF RESPONSIBLE INDIVIDUAL Theodore E. Luke, Professor		22b. TELEPHONE (Include Area Code) (513) 255-4498	22c. OFFICE SYMBOL AFIT/ENP